THE ROLE OF PERIOSTIN IN THE PROGRESSION OF CLEAR CELL RCC

THE ROLE OF PERIOSTIN IN PROMOTING THE PROGRESSION OF CLEAR CELL RENAL CELL CARCINOMA

By

NAZIHAH BAKHTYAR, B.Sc. (Hons)

A Thesis

Submitted to the School of Graduate Studies

In Partial Fulfillment of the Requirements

for the Degree

Master of Science

McMaster University

McMaster University MASTER OF SCIENCE (2013) Hamilton, Ontario (Medical Sciences)

TITLE: The Role of Periostin in Promoting the Progression of Clear Cell Renal Cell Carcinoma

AUTHOR: Nazihah Bakhtyar, B.Sc. (Hons.) (McMaster University)

SUPERVISOR: Dr. Damu Tang

NUMBER OF PAGES: xii, 87

ABSTRACT

Renal cell carcinoma (RCC) is the third most common genitourinary cancer after the cancers of prostate and bladder. The majority (75%) of RCC is comprised of clear cell renal cell carcinoma (ccRCC). Despite ccRCC being the most aggressive form of RCC, our knowledge regarding the pathogenesis of the disease remains limited. To advance our understanding of ccRCC pathogenesis, we have identified upregulation of the extracellular protein periostin (POSTN) in ccRCC. Western blot analysis of ccRCC tumours from 27 patients demonstrated high POSTN protein expression in 26 tumours compared to their respective adjacent normal kidney tissue (ANK). While immunohistochemistry (IHC) analysis revealed low levels of POSTN in the tubular epithelial cells of the ANK tissues, high levels of stromal POSTN protein were observed in the ccRCC tumours. Elevated stromal POSTN was also demonstrated in 16 metastasized ccRCCs. Intriguingly, abundant stromal POSTN in the boundary between the tumour mass and non-tumour tissues were observed in local and metastaized ccRCC, and in A498 ccRCC cell-derived xenograft tumours. Collectively, these results suggest that the ccRCC-associated POSTN was derived from the stroma. This notion was supported by the co-existence of POSTN with α-smooth muscle actin (αSMA) in both local and metastasized ccRCC tumours. αSMA is a marker of activated fibroblasts (myofibroblasts), the major cellular components of stroma. Furthermore, co-culture of NIH3T3 murine fibroblasts with human A498 or 786-0 ccRCC cells dramatically enhanced POSTN transcription and secretion from NIH3T3 cells. Extracellular POSTN significantly enhanced A498 cell attachment. Upregulation of POSTN in NIH3T3 cells

enhanced their proliferation. Taken together, my research demonstrates that 1) ccRCC induces fibroblast-mediated accumulation of extracellular POSTN, 2) stromal POSTN enhances ccRCC attachment, and 3) high levels of POSTN promotes fibroblasts' proliferation. These observations suggest a critical role for POSTN in mediating the co-evolving process between ccRCC and its stroma during ccRCC pathogenesis.

ACKNOWLEDGEMENTS

I would like to start by thanking my supervisor Dr. Damu Tang. Thank you so much for this opportunity to conduct research in your lab, for your guidance, encouragement and wise words. Your office door was always open if I wanted to discuss my research, and you helped me achieve a higher level of thinking with regards to science. I would like to thank my committee members Dr.Michelle Ghert and Dr.Darren Bridgewater. Thank you for all of your suggestions over the duration of my Master's studies, and for taking the time to help me improve my thesis draft.

I would like to thank all of the students in Dr.Tang's lab for their technical and motivational support over these past few years.

Last but definitely not least; I would like to acknowledge my parents. Your continuous love and support has made this journey possible. I want to thank you for everything that you do for me.

TABLE OF CONTENTS

LIST OF TABLES

IV: MATERIALS AND METHODS

LIST OF FIGURES

LIST OF ABBREVIATIONS

ANK	Adjacent non tumour kidney
bFGF	Basic fibroblast derived growth factor
ccRCC	Clear cell renal cell carcinoma
ECM	Extracellular matrix
EGF	Epidermal growth factor
ELISA	Enzyme linked immunosorbent assay
FAS 1	Fascilin 1
GP	Gag pol expression vector
GSK3β	Glycogen synthase kinase 3 β
GST	Glutathione S transferase
HIF1α	Hypoxia-inducible factor α
IF	Immunofluorescence
IHC	Immunohistochemistry
IFN-α	Interferon alpha
IL2	Interleukin 2
MMP	Matrix metalloproteinase
mTOR	Mammalian target of rapamycin
PBS	Phosphate buffer saline
PDGF	Platelet derived growth factor
PI3K	Phosphatidylinositol-3 kinase
POSTN	Periostin
pRCC	Papillary renal cell carcinoma
qRT-PCR	Quantitative real time polymerase chain reaction
RCC	Renal cell carcinoma
RPM	Rotations per minute

αSMA	alpha smooth muscle actin
TGFβ	Transforming growth factor β
VEGF	Vascular endothelial growth factor
VHL	von hippel-lindau
VSV-G	Vesicular stomatitis virus G protein

I. INTRODUCTION

1.1. Renal Cell Carcinoma

Renal cancer affects 32,000 Americans annually and it is linked with almost 12,000 deaths in the United States every year (Linehan *et al*., 2001; Landis *et al*., 1999). Kidney cancer is a heterogenous disease, consisting of primary neoplasms of the renal pelvis or ureter (7-8%), Wilms tumour (5-6%), and Renal cell carcinoma (RCC, 85%). Wilms tumour is a pediatric cancer, which is derived from pluripotent embryonic renal precursors (Lee & Haber, 2001). The incidence of Wilms tumour is approximately 1 in 10,000 children and the cure rate is approximately 80% (Lee & Haber, 2001).

RCC is the third most common genitourinary cancer after that of prostate and bladder (Jemal *et al*., 2002) and it represents 3% and 4% of newly diagnosed malignancies in adult females and males respectively (Jemal *et al*., 2008). RCC consists of multiple epithelial neoplasms of the kidney and each form is associated with a set of different genetic alterations. Clear cell renal cell carcinoma (ccRCC, 75%) is associated with the loss of the *Von Hippel Lindau (VHL)* tumour suppressor gene. Papillary type 1 and type 2 RCC (15%) are associated with changes in the *MET* and the *fumarate hydratase (FH)* gene. Chromophobe RCC (5%) and oncocytoma (5%) are both affiliated with abnormalities in the *Birt Hogg Dube (BHD)* gene (Fig 1A) (Linehan *et al*., 2003).

Clear cell RCC is the most aggressive form of RCC . Approximately 40-45% of ccRCC cases have locally advanced or metastatic cancer at time of diagnosis and 30% of initially organ-confined cases will develop metastases (Nelson *et al*., 2007; Uchida *et al*., 2002; Levy *et al*., 1998). Currently, therapeutic options for metastasized ccRCC are very limited and metastasized ccRCC remains a lethal disease. While patients with localized ccRCC have a good prognosis, those with advanced cancer have a dramatically decreased rate of survival. Five and 10-year survival is approximately 95% for stage I, 88 -81% for stage II, 59 - 43% for stage III, and 20-14% for the stage IV disease (Javidan *et al*., 1999). ccRCC is also notoriously resistant to chemotherapy and radiotherapy (Yagoda *et al*., 1995). The chemoresistance of ccRCC is attributed to the high expression of multiple drug resistance (MDR-1) gene products such as P-glycoprotein (80% of RCC) as well as the high levels of glutathione (Mickisch *et al*., 1994; Liu *et al*., 2001).

ccRCC was defined by the World Health Organization (WHO) in 2004 as a malignant renal neoplasm comprised of cells with a clear or eosinophilic cytoplasm and a fine vascular system (Grignon *et al*., 2004). The tumour is usually a solid mass with a yellowish golden manifestation due to the presence of large amounts of lipid in the tumour (Fig1B) (Grignon & Che, 2005). Under the microscope, the cells display transparent cytoplasm with defined cell borders. The cytoplasm contains glycogen and lipids which are dissolved during histological preparation, allowing the cytoplasm to appear clear, or eosinophilic if it is of higher grade (Lam *et al*., 2005). ccRCC originates from the proximal convoluted tubule of the nephron.

1.2. Presentation and Diagnosis of ccRCC

Renal cell carcinoma occurs more in males than females. The onset of disease usually occurs at a median age of 60 (Nelson *et al*., 2007). Some local signs and

A.

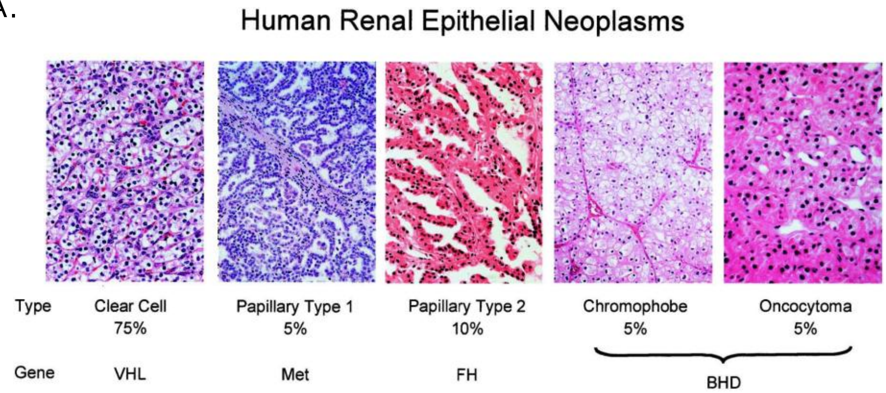

(Linehan *et al.*, 2003)

B.

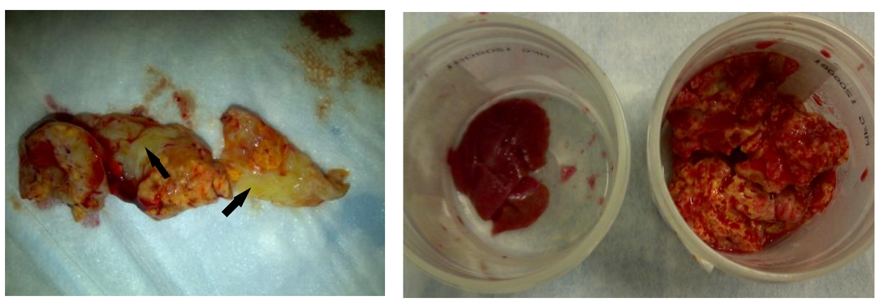

Figure 1. Renal cancer. **A)** Different types of human renal epithelial cancers with percentage of occurrence and associated genetic alteration (Linehan *et al.*, 2003). **B)** Left image is an example of a renal tumour, the arrows point to the clear cell variant of renal cell carcinoma. Image on the right displays a normal kidney section in the container on the left and a renal tumour in the container on the right.

symptoms of ccRCC include haematuria, flank pain, or a palpable abdominal mass (Nelson et al., 2007). A ccRCC patient may also display systemic symptoms as a result of secreted proteins, including parathyroid hormone-related protein (causing hypercalcaemia), renin (causing hypertension) or erthyropoietin (causing erythrocytosis) (Nelson *et al*., 2007). The secretion of such proteins is a secondary effect due to the presence of the renal tumour. Currently, the frequent use of ultrasonography and cross sectional imaging is linked with incidental detection of asymptomatic renal tumours (Rini *et al*., 2009). Tumour staging is carried out primarily with computed tomography (CT), which allows for the determination of local invasiveness, lymph node involvement, or other metastases (Rini *et al*., 2009).

The prognosis for ccRCC is mainly dependent on the clinical stage and nuclear grade (Amin *et al*., 2002). In comparison to papillary and chromophobe RCC, the prognosis for ccRCC is quite poor. The nuclear characteristics of ccRCC cells are used to determine ccRCC behavior and progression. There is a four tiered nuclear grading system used to define ccRCC which has been developed by Fuhrman *et al.*, and is referred to as the Fuhrman nuclear grade (Fuhrman *et al*., 1982).

1.3. Treatment Strategies for ccRCC

If ccRCC is detected at an early stage, surgery is a viable option for its removal through either radical or partial nephrectomy (Lam *et al*., 2004; Fergany *et al*., 2000). If the cancer has spread to secondary locations, surgery must be followed with further treatment. Some of the most common sites of metastasis for ccRCC are the lungs, liver, lymph node and bone. Other sites include the pancreas, adrenal gland, the contralateral kidney and the brain (Prasad *et al*., 2006; Brant *et al*., 1999; Lin *et al*., 2007). Patients with metastasized ccRCC have a poor prognosis owing to its resistance to the currently available therapies. Clear cell RCC can induce an immune response that regulates the growth of metastatic tumour. Consequently, immunotherapeutic agents such as interleukin 2 (IL2) and interferon alpha (IFN-α) have been used to treat metastatic ccRCC, but with limited success. In addition, both IL2 and IFN-α are associated with severe side effects (Prenen *et al*., 2009).

Recent development allows patients with metastatic ccRCC to undergo targeted therapies. The principle behind targeted therapies is the dependence of tumour cells on specific biological pathways. One of the most common pathways targeted is the vascular endothelial growth factor (VEGF) pathway. VEGF is a potent growth factor that plays an essential role in angiogenesis in tumours including ccRCC. There are two main approaches to hinder the VEGF pathway. One is to inhibit the tyrosine kinase activity of the VEGF receptor using tyrosine kinase inhibitors, including sunitinib, sorafenib, axitinib, and pazopanib (Prenen *et al*., 2009). Another approach is to prevent VEGF from binding to its receptor by using monoclonal antibodies to neutralize VEGF. One such drug is bevacizumab. The mTOR (mammalian target of rapamycin) pathway is also being targeted. mTOR is a serine/threonine kinase that regulates cell survival and angiogenesis. The drugs used to inhibit the mTOR pathway include rapamycin, temsirolimus and everolimus (Prenen *et al*., 2009). These drugs have been or are currently being tested in clinical trials. A randomized phase III trial comparing sunitinib to IF-α as a first line of treatment for advanced RCC had a 31% response rate for the sunitinib arm versus 6% for IF-α. Progression free survival was 11 months for sunitinib and 5 months for IF-α. On January 26, 2006 the Food and Drug Administration (FDA) approved sunitinib as a first line treatment for advanced RCC (Prenen *et al*., 2008). However, despite these advances in targeted therapies, metastatic ccRCC still remains an incurable disease.

1.4. The Genesis of ccRCC

ccRCC results due to the accumulation of mutations in oncogenes or tumour suppressor genes. These mutations can be either sporadic or hereditary. Mutations in tumour suppressor genes located in three specific regions on chromosome 3p have been identified in patients with ccRCC. The translocation t(3;8) involves 3p12-p14, a region that is associated with hereditary ccRCC and contains a putative tumour suppressor gene, the *FHIT* (fragile histidine triad) gene. The deletion of 3p21.2-p21.3 occurs frequently in many cancers including cancer of the kidney and the lung. The third altered region involves 3p25-p26 which contains the *von Hippel–Lindau (VHL)* tumour suppressor gene. Mutation in the *VHL* gene is an early event in ccRCC pathogenesis (Clifford *et al*., 1998).

Individuals with one wild type *VHL* and one inactivated *VHL* allele suffer from VHL disorder (Kim & Kaelin, 2004). VHL disorder affects many organs, with kidneys being the major one. Individuals with VHL disease are at risk for the development of renal cysts due to inactivation of the wild type *VHL* allele. These cysts can progress to ccRCC (Rini *et al*., 2009). Germ line mutations of the *VHL* gene have been found in almost all families with *VHL* disorder, allowing it to become most frequent cause of hereditary ccRCC (Linehan *et al*., 2010). Somatic inactivation of VHL by hypermethylation or mutation has been reported in up to 91% of sporadic ccRCC cases (Linehan *et al*., 2010). The VHL protein complex targets the hypoxia inducible factor 1-α (HIF1-α) transcription factor for ubiquitin-mediated degradation. Loss of VHL leads to the stabilization of HIF1-α , which transactivates multiple target genes, including VEGF, the glucose transporter (GLUT 1), platelet derived growth factor (PDGF), transforming growth factor-β (TGF-β) and erythropoietin (EPO) (Linehan *et al*., 2003). These proteins promote tumorigenesis via enhancing angiogenesis, cell survival and cell proliferation.

In addition to the tumour suppressor genes residing on chromosome 3p, abnormalities in other chromosome regions also contribute to ccRCC tumorigenesis, including the gain of chromosome 5p and loss of chromosome 8p, 9p and 14q (Martinez *et al*., 2000; Rini *et al*., 2009). This knowledge is consistent with the observation that inactivation of VHL is not sufficient in inducing ccRCC (Rini *et al*., 2009).

1.5. The Role of Cancer Associated Stroma in Tumour Progression

A solid tumour is a heterogeneous mass, consisting of tumour and stromal cells. Tumorigenesis is a co-evolved process between the tumour and its stroma, where there exists cross talk between the different types of cells in the tumour mass (Mueller & Fusenig, 2004). The stromal cells include fibroblasts, immune and inflammatory cells and blood vessel cells (Tlsty & Coussens, 2006). The fibroblasts comprise the majority of the stromal cells (Tlsty & Coussens, 2006).

The fibroblast cells can be activated into myofibroblasts. This transition is an indication of the stroma becoming modified due to the presence of cancer cells (De Wever *et al*., 2000; Sappino *et al*., 1990). A typical characteristic of myofibroblasts is the acquisition of α smooth-muscle-actin (αSMA) expression. It has been reported that the acquisition of αSMA in myofibroblasts is a result of signaling between epithelial cancer cells and stromal cells (Desmouliere *et al*., 2004). Myofibroblasts secrete soluble factors such as extracellular matrix (ECM) components [collagen, tenascin, fibronectin and matrix mettaoproteinase (MMP)]. These ECM proteins induce matrix remodeling (Tuxhorn *et al*., 2002; Hanamura *et al*., 1997). Myofibroblasts also secrete growth factors and cytokines that act in a paracrine manner on cancer cells and stromal cells (Rasanen & Vaheri, 2010). The production of such factors results in a pro migratory, pro invasive and a pro angiogenic environment (Mueller & Coussens, 2004).

Cancer cells can influence the formation of a tumour supportive environment by secreting factors which modulate the stroma. Some of these factors include: basic fibroblast growth factor (bFGF), VEGF, PDGF, epidermal growth factor (EGF), TGFβ and others (Mueller & Fusenig, 2004).

The communication between malignant cells and their microenvironment is an important aspect of tumorigenesis, not only for tumour maintenance but also for initiating metastases. Metastasis occurs through a systematic process. Primary tumour cells first detach from the extracellular matrix and enter the systemic circulation by infiltrating thin walled vessels. Tumour cells then travel to secondary sites and extravasate by multiple mechanisms into the underlying tissue parenchyma. The initiation of a growth at the secondary location requires tumour cells to interact with the matrix proteins in the stroma and establish an environment for their growth (Langley & Fidler, 2011). This interaction involves the heterodimeric cell surface integrin proteins. The binding of matrix proteins to integrins leads to matrix remodeling, cell migration and also the induction of intracellular signaling cascades (Zigrino *et al*., 2004).

1.6. Periostin

POSTN is a disulfide linked 90 kDa N glycoprotein secreted by osteoblasts and osteoblast-like cell lines (Takeshita *et al*., 1993). POSTN was initially identified in screening a cDNA library that was established from the mouse osteoblastic cell line MC3T3-E1, in an attempt to identify genes that were specifically expressed in osteoblasts (Takeshita *et al*., 1993). A cDNA was isolated, which encoded the osteoblast specific factor 2 (OSF-2) (Takeshita *et al*., 1993). This protein functions as a bone adhesion molecule responsible for differentially recruiting and attaching osteoblasts to the periosteum and was subsequently renamed as POSTN. POSTN contains a NH2 terminal signal peptide, a cysteine rich domain (EMI domain) first named after its presence in proteins of the EMILIN family, a fourfold fascilin 1 (FAS1) homologous repeat domain and a hydrophilic C terminal domain (Fig 2A). POSTN is a secreted cell adhesion protein with two functional regions, the FAS1 domains and the C terminal domain. The FAS1 repeats are homologous to the insect axon guidance fasciclin I domain and β-IgH3 in humans (Takeshita *et al*., 1993). The β-IgH3 protein is induced by TGFβ and bone morphogenetic protein-2 (BMP-2), and plays a role in supporting the adhesion and spreading of fibroblasts (Horiuchi *et al*., 1999). The FAS1 domain of POSTN interacts with cellular integrins (Orecchia *et al*., 2011; Morra & Mock, 2011).

Integrins are transmembrane heterodimeric receptor complexes involved in both cell to cell and cell to extracellular matrix interactions where they can transmit "outside in" signals to cells (Gillan *et al*., 2002). Integrins not only play a role in cell adhesion but are also involved in the activation of cytosolic signaling cascades to mediate cell proliferation, cell survival, and cell migration. In cancer cells, integrin expression is frequently altered, and hence, with the changes in the ECM composition in tumours, the adhesion characteristics and motility of cancer cells is also modified (Gillan *et al*., 2002). POSTN regulates cell-matrix organization and ECM remodeling by interacting with ECM proteins such as collagen V, fibronectin, tenascin-C as well as well as POSTN itself (Norris *et al*., 2007; Kii *et al*., 2010). It has been reported that the C terminal domain of POSTN plays a role in such interactions (Takayama *et al*., 2006; Kii *et al*., 2010). In adult mice, POSTN is mainly expressed in the periosteum and periodontal ligaments. Therefore, POSTN plays a critical role in bone and teeth formation and maintenance (Horiuchi *et al*., 1999). POSTN is also involved in the development of the heart and certain pathological conditions of the heart. The mouse and human POSTN protein exhibit high amino acid sequence conservation except for the signal and the C terminal sequence (Takeshita *et al*., 1993). Nucleotide sequence revealed that POSTN transcripts differ in the length of the C-terminal domain, indicating alternative splicing events (Fig 2B).

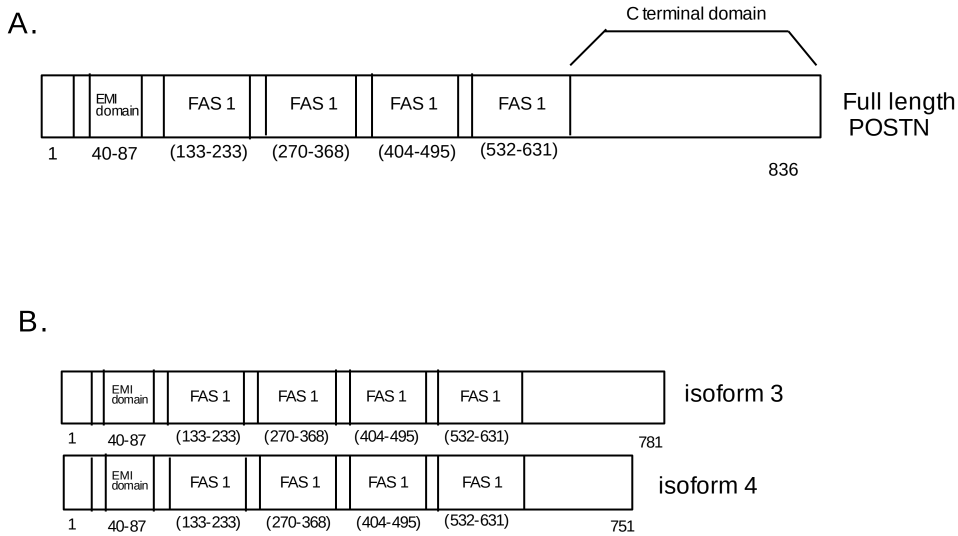

Figure 2. Schematic of periostin protein with examples of two splice variants detected in renal cancer. Numbers represent amino acid number. **A)** POSTN protein schematic. After the N terminus is the EMI cysteine rich domain, followed by four homologous FAS1 repeats. The C terminal domain length varies depending on splicing events. **B)** Examples of POSTN splice variants detected in renal cancer.

Over the past decade, a critical role for POSTN has been established in cancer biology. POSTN is overexpressed in human cancers such as lung (Soltermann *et al*., 2008; Morra *et al*., 2012), esophagus (Michaylira *et al*., 2010), colon (Bao *et al*., 2004), liver (Utispan *et al*., 2010; Fujimoto *et al*., 2011), pancreas (Baril *et al*., 2007; Ben *et al*., 2011), thyroid (Puppin *et al*., 2011), ovary (Gillian *et al*., 2002; Zhu *et al*., 2010), breast (Shao *et al*., 2004; Puglisi *et al*., 2008), and prostate (Tsunoda *et al*., 2009; Tischler *et al*., 2010).

1.7. Periostin Expression Patterns in Tumours

POSTN expression and localization varies amongst cancers. A 20 fold increase in POSTN mRNA in breast tumour was observed when compared to normal breast tissue. IHC revealed that POSTN was predominantly localized in the carcinoma cells, which suggested that POSTN was originated from the breast tumour cells (Shao *et al*., 2004). In comparison to xenograft tumours produced from control MDA-MD-231 breast cancer cells, two to four fold higher blood volume were detected within the xenograft tumours generated from MDA-MD-231 over expressing POSTN. It was reported that POSTN promoted angiogenesis via upregulation of the VEGF receptor Flk-1/KDR (Shao *et al*, 2004).

Recently, stromal POSTN was reported to play a role in maintaining niches for breast cancer stem cells during metastasis by enhancing metastatic colonization in a breast cancer mouse model (Malanchi *et al*., 2012). Via RNA situ hybridization and IHC, it was demonstrated that in breast tumours stromal POSTN was produced by fibroblast cells which were positive for alpha smooth muscle actin (SMA) and vimentin. Additionally, co-culture of fibroblasts with breast cancer cells resulted in upregulation of POSTN by fibroblasts (Malanchi *et al*., 2012). Furthermore, infiltrating breast tumour cells induced the stromal production of POSTN. This POSTN expression in turn determined cancer stem cell maintenance and metastatic efficiency. Consistent with cancer stem cells being responsible for the origin of metastasis, stromal POSTN was found to be critical in maintaining niches for breast cancer stem cell (Malanchi *et al*., 2012).

In prostate cancer, stromal POSTN expression was detected in high grade tumours (Gleason score 8-10) as compared to lower grade (gleason score 6-7) tumours. The stromal expression of POSTN correlates with degree of malignancy in prostate cancer (Tsunoda *et al*., 2009).

1.8. Periostin Induced Cancer Associated Molecular Pathways

A critical pathway involved in cancer development is the phosphatidylinositol-3 kinase (PI3K) pathway (Vivanco *et al*., 2002) (Fig 3A). PI3K activation is countered by the PTEN tumour suppressor. AKT is an important component of the PI3K pathway and its activation has been reported to transform cells (Staal *et al*., 1988). AKT was identified as an oncogene in 1988 owning to the observation that AKT8 virus was able to transform cells in vitro. Upregulation of the *AKT1* gene has been reported in human gastric adenocarcinoma (Staal *et al*., 1988). AKT activation results in activation of mammalian target of rapamycin (mTOR) which in turn leads to the activation of p70 S6 kinase and

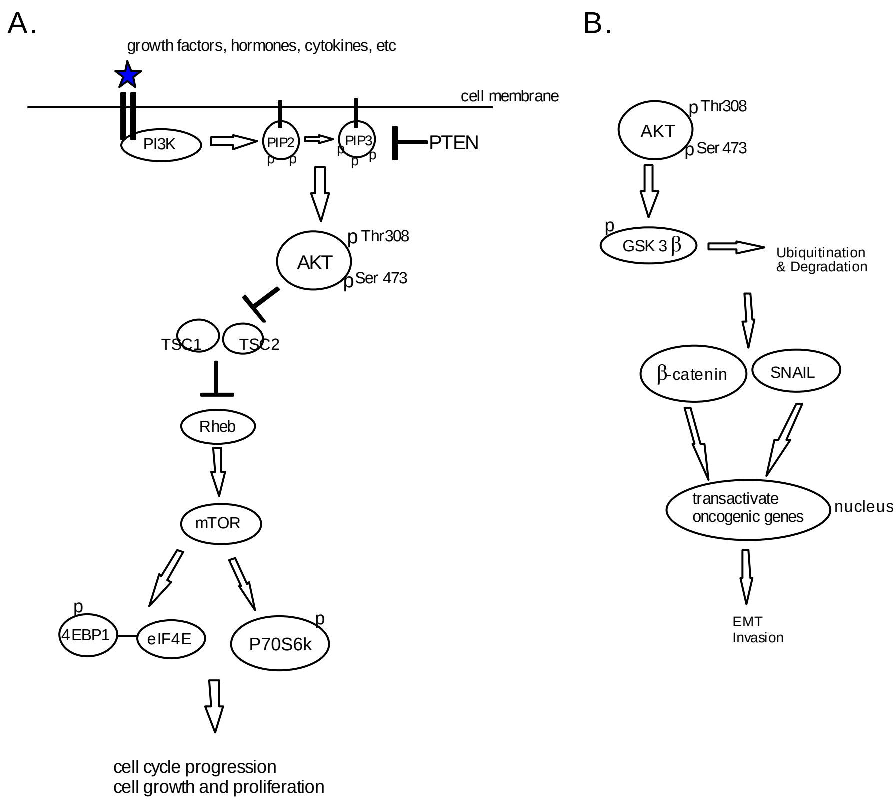

Figure 3. Schematic of PI3K/AKT pathway and GSK3β inactivation by AKT. **A)** Activation of the receptor tyrosine kinase leads to recruitment of PI3K to the membrane. Activation of PI3K leads to the phosphorylation of PIP2 into PIP3. PIP3 recruits AKT to the membrane and AKT activation leads to downstream activation of mTOR. PTEN is a suppressor of this pathway. p-AKT inhibits the TSC complex which inhibits mTOR activation. Rheb is suppressed by TSC complex, but when released it can activate mTOR. mTOR actiavtion leads to the activation of P70S6K and release of the 4EBP1-eIF4E complex. P70S6K activation and eIF4E release from its complex leads to the promotion of the cell cycle from cell cycle arrest and initiates protein synthesis (Vivanco et al., 2002). **B)** Activated AKT can also phosphorylate GSK3β and cause it to become ubiquitinated and degraded. This leads to the transport of either β-catenin or SNAIL to the nucleus where they can upregulate a variety of oncogenic genes for tumour development and metastases (Qiao *et al*., 2008).

release of eukaryotic initiation factor 4E (elF4E) from 4E-BP1, elF4E can go on to initiate translation. The combination of these two events induces protein synthesis and thereby promotes cell proliferation (Vivanco *et al*., 2002). In addition, AKT also inactivates the glycogen synthase kinase 3 β (GSK-3β) tumour suppressor by phosphorylating its Ser-9 residue. This leads to ubiquitination and degradation of GSK3 β. Loss of GSK-3β results in the stabilization of β-Catenin and SNAIL, which are subsequently translocated to the nucleus to transactivate oncogenic genes in a variety of tumour settings (Fig3B) (Qiao *et al*., 2008). AKT can also regulate Bcl-2-associated death promoter (Bad), Caspase 9, Tuberin, and a group of forkhead transcription factors that regulate cell growth, differentiation and proliferation. Therefore, AKT activation regulates multiple cellular processes involved in cell proliferation, cell survival, invasion and angiogenesis (Vivanco *et al*., 2002; Cantley, 2002; Yardena *et al*., 2006).

POSTN was reported to promote cell survival. POSTN overexpression in CX-1NS colon cancer cells led to the activation of the AKT pathway in comparison to control cells (Bao *et al*., 2004). Moreover, recombinant POSTN also induced AKT activation in CX-1NS colon cancer cells or human microvessel endothelial cells (HMVECs). POSTN activated AKT in these cells via binding to the αvβ3 integrin (Bao *et al*., 2004). AKT activation prevented these cells from stress-induced apoptosis. Conversely, inhibition of ATK activation by using either an AKT inhibitor or PTEN overexpression abolished POSTN's ability to protect cells from stress-induced cell death (Bao *et al*., 2004).

Consistent with the above report, POSTN activates the focal adhesion kinase (FAK) by binding to integrins (Baril *et al*., 2007). It is well established that ligand-binding to integrin activates FAK, which in turn activates AKT to mediate cell spreading. Consistent with this knowledge, immobilized POSTN induces the phosphorylation of FAK at tyrosine 397 and AKT activation via binding the β4 integrin (Baril *et al*., 2007).

POSTN also plays a role in hypoxia-induced AKT activation. Under hypoxia, recombinant POSTN induces AKT activation in CFPac1 pancreatic adenocarcinoma cells (Baril *et al*., 2007). POSTN-induced AKT activation was sensitive to PI3K inhibitors LYP29002 and wortmanin but not the MEK inhibitor PD98059, providing evidence that POSTN activates AKT via facilitating PI3K activation. In line with these results, POSTN was found to activate PI3K via its action on the p85 subunit of the PI3K complex. Collectively, recombinant POSTN activates AKT by facilitating PI3K activation (Baril *et al*., 2007).

1.9. Periostin Expression in ccRCC

In an effort to isolate kidney cancer antigens, Castronovo and his colleauges identified POSTN as the most abundant tumour-associated antigen by using a chemical-based proteomics approach (Castronovo *et al*., 2006). However, the most thorough study on the involvement of POSTN in ccRCC was reported by Morra and his lab in 2011. For the purpose of screening POSTN isoforms specifically expressed in ccRCC, total mRNA from a cohort of 30 patient's fresh frozen RCC tissues, normal kidney tissues as well as fetal kidney tissues were obtained. PCR reaction covering the exons 14-23 revealed the presence of 8 isoforms. Among them, isoforms 5-8 were newly identified. Isoforms 3, 4 and 8 were detected in RCC and the corresponding normal tissue, whereas full length

POSTN as well as isoforms 2, 5, 6 and 7 were only present in fetal kidney. Isoform 8, missing exons 17, 18, 19 and 21 was the novel ccRCC isoform discovered. Analysis of 30 RCC samples detected POSTN in the cytoplasm of both tumour and stromal fibroblast cells (Morra *et al*., 2011).

II. HYPOTHESIS

The role of POSTN in the pathogenesis of ccRCC remains unclear. In different human cancers, elevated levels of POSTN were reported in tumour or stromal cells. At the time when this project was initiated, the exact location and origin of POSTN in ccRCC remained unknown. In our effort to examine the POSTN protein in ccRCC versus its ANK, we noticed a robust upregulation of POSTN in ccRCC. Similar observations were reported by other groups (Morra *et al*., 2011). Nonetheless, we observed high levels of stromal POSTN and whether POSTN was derived from the tumour or stromal cells remained unclear. In addition, the impact of stromal POSTN on tumour and stromal cells in ccRCC is unknown. In this context, my central hypothesis is that during ccRCC pathogenesis increased POSTN is accumulated in the tumour stroma and that high levels of stromal POSTN impact tumour cells and stromal cells to favor ccRCC pathogenesis. To address this hypothesis, the major objectives of this research are as follows:

Aim 1. I will thoroughly analyze POSTN protein expression by western blot and IHC analysis using human ccRCC tissues from our RCC tissue bank. This research will build a strong foundation regarding the POSTN protein levels in ccRCC versus its ANK.

Aim 2. As there is no report regarding POSTN expression in metastasized ccRCC, we will determine POSTN protein expression in metastasized ccRCC. In comparison to the local ccRCC, this research will advance our knowledge regarding the potential involvement of POSTN in ccRCC metastasis.

Aim 3. Since POSTN is an extracellular matrix protein, its extracellular accumulation can be attributable to either tumour or stromal cells. The origin of the stromal POSTN in ccRCC will be determined.

Aim 4. POSTN has been reported to enhance cell survival and proliferation. The high levels of stromal POSTN observed in ccRCC may affect the biology of tumour and stromal cells. I will examine the potential impact of POSTN on the stromal cells.

III. MATERIALS AND METHODS

3.1. Reagents

Ampicillin, ammonium per sulphate (APS),calcium chloride ($CaCl_2$), crystal violet dimethyl sulfoxide (DMSO), ethidium bromide, EDTA, aprotinin, leupeptin, phenylmethylsulfonyl fluoride (PMSF), β-glycerophosphate, Triton X-100, Tween 20, β-mecaptoethanol, puromycin, bromophenol blue, ammonium per sulphate (APS), iodacetamide, sodium bicarbonate ($CHNaO_3$), Carbonate (Na_2CO_3), puromyocin, potassium dihydrogen orthophosphate (KH_2PO_4), disodium hydrogen orthophosphate (Na_2HPO_4), glycerol, thiourea and GenElute Plasmid Miniprep kit were purchased from Sigma, Oakville, ON. Agarose, bovine serum albumin (BSA), Tris base, glycine, sodium dodecyl sulphate (SDS), sodium citrate, sodium chloride (NaCl), TEMED were purchased from Bioshop Burlington, ON. Trypsin-EDTA was purchased from Invitrogen, Carlsbad, CA. 30% Bis Acrylamide solution, Biolytes 3/10, Urea, CHAPS and IPG strips was purchased from Bio-Rad, Mississauga, ON. Methanol and isopropyl alcohol were purchased from Caledon Laboratories, Georgetown, ON and reagent alcohol was purchased from Fisher Scientific, Ottawa, ON. Anhydrous Ethyl Alcohol was purchased from Commercial Alcohols, Brampton, ON. Ultraclean 15 DNA purification kit was purchased from MoBio Laboratories Carlsbad, CA.

3.2. Cell Lines and Antibodies

3.2.1 Cell lines

293T human embryonic kidney cells, NIH3T3 murine fibroblast cells, and human ccRCC cell lines 786-O, 1933, and A498 were purchased from American Type Culture Collection (ATCC, Manassas VA) and cultured in RPMI 1640, MEM, DMEM media supplemented with 10% fetal bovine serum and 1% Penicillin-Streptomycin (Invitrogen, Burlington ON). The cells were grown in a $37^{o}C$ and 5% CO_2 tissue culture incubator.

3.2.2 Antibodies

Antibodies used for western blotting, IHC and IF were rabbit anti-POSTN (Abcam, Cambridge MA), mouse anti-flag M2 (Sigma, Oakville ON), rabbit and mouse anti factor VIII (Graciously provided by Dr.Peter Margett's lab. Dako, Burlington ON), rabbit anti-phospho AKT (Cell Signaling, Danvers MA), goat anti-AKT (Santa Cruz, Santa Cruz CA),rabbit anti-phospho GSK (Cell Signaling, Danvers MA), mouse anti-GSK (Santa Cruz, Santa Cruz CA), rabbit anti-phospho P70S6K (Cell Signaling, Danvers MA), rabbit anti-P70S6K (Cell Signaling, Danvers MA), mouse anti-αSMA (Dako, Burlington ON), mouse anti-fibronectin (Cell Signaling, Danvers MA), goat anti-actin (Santa Cruz, Santa Cruz CA). Secondary antibodies for western blot (anti-rabbit IgG and anti-mouse IgG) were purchased from Amersham and anti-goat IgG was purchased from Santa Cruz Biotechnology. Secondary antibodies for IHC were purchased from Vector Laboratories (Burlingame, CA).

3.3. Collection of Primary and Metastatic RCCs

46 pairs of primary RCC and their respective non-tumour kidney tissues were collected in compliance with the local ethics regulations at St. Joseph's Healthcare Hamilton, Ontario, Canada. The pathological diagnoses were performed by the pathologists of the hospital. All ccRCCs, pRCCs and their non-tumour kidney tissues were confirmed by H&E staining (Table 1 and 2). Approval from McMaster Health Science research ethics board (REB) and St.Joseph's Healthcare Hamilton REB allowed for the systematic search through patient databases spanning 20,000 cases to obtain metastatic ccRCC. 16 cases of metastatic ccRCC to secondary organs were located, the paraffin embedded tissue blocks were pulled and slides were cut (Table 3).

3.4. Protein Analysis

3.4.1 Cell Lysate Preparation

Cells lysates were prepared by washing the cells twice with phosphate buffered saline (PBS) on ice (PBS: 1.36 M NaCl, 14.7 mM KH_2PO_4, 80mM Na_2HPO_4, 26.8mM KCl pH 7.2), harvesting cells in PBS using a cell scraper, and centrifugation at 2000rpm at 4^{o}C for 5 minutes. PBS was aspirated and the cell pellet was resuspended in lysis buffer (20 mM Tris-HCl pH 7.4, 150 mM NaCl, 1 mM EDTA, 1 mM EGTA, 1% Triton X-100, 25 mM sodium pyrophosphate, 1 mM NaF, 1 mM β-glycerophosphate, 0.1 mM sodium orthovanadate (Na_3VO_4), 1 mM PMSF, 2 µg/ml leupeptin and 10 µg/ml aprotinin) for 30 minutes on ice. The lysates were then centrifuged at 13,000rpm at 4^{o}C for 5 minutes. The supernatant was collected and protein concentration was determined using a Bradford assay (Bio-Rad, Mississauga, ON). Absorbance was measured at 595nm

Table 1: ccRCC Patient Information

Patient	Age	Gender	Pathology	FG[1]	Metastasis[2]	Volume cm^3	POSTN Below 83kDa T/N[4]	Experiment [5]
22	75	F	ccRCC	3	No	1089		I
23	38	M	ccRCC	2	No	18.85		I,IF
40	63	M	ccRCC	2	No	560.625		I
29	63	M	ccRCC	3	No	72		I/IF
38	63	M	ccRCC	3	No	17.5		I,IF
48	58	M	ccRCC	2	No	86.4		I
30	70	F	ccRCC	1	No	42	1.388038	I,IF,W
66	51	M	ccRCC	1	No	50.49	4.673792	I,W
67	54	F	ccRCC	1	No	17.856	10.55552	I,E,W
68	77	F	ccRCC	2	No	99		E
72	45	M	ccRCC	3	No	47.25		E
73	41	F	ccRCC	1	No	93	0.267315	E,W
75	68	M	ccRCC	3	No	148.5	23.0296	E,W
80	55	M	ccRCC	4	No	936		E
81	76	M	ccRCC	2	Yes -bone	170.5		E
83	68	F	ccRCC	2	No	26.25	1.744197	E,W
89	59	M	ccRCC	2	No	5.5*5.0	7.15292	E
90	49	F	ccRCC	2	No	5*4.9	4.737116	E,W
91	43	M	ccRCC	2	No	3	2.503244	E,W
100	50	M	ccRCC	1	No	3.825	6.775723	E,W
105	83	F	ccRCC	2	No	336	1.108634	E,W
106	N/A[3]		ccRCC			N/A[3]	1.295034	E,W
107	56	F	ccRCC	3	No	N/A[3]	2.297656	E,W
108	71	M	ccRCC	3	No	812.5	12.84093	E,W
111	67	F	ccRCC	2	No	N/A[3]	1.97725	E,W
112	62	M	ccRCC	3	No	N/A[3]	4.289087	E,W
119	N/A[3]	F	ccRCC	2	No	N/A[3]	17.36574	E,W
126	48	F	ccRCC	2	No	N/A[3]	19.48896	E,W
127	62	M	ccRCC	3	No	24.5	1.465873	E,W
130	75	M	ccRCC	2	No	96	5.891493	E,W
139	45	F	ccRCC	1	No	15.4	22.63167	W
144	48	M	ccRCC	1	No	N/A[3]	20.67812	W
145	62	M	ccRCC	2	No	N/A[3]	2.31878	W
146	53	F	ccRCC	1	No	63	7.53056	W
95	68	M	ccRCC	3	No	72.9	3.014805	W
69	48	M	ccRCC	3	No	1039.5	3.246288	W
77	57	M	ccRCC	3	Yes	445.5	2.367212	W

1: FG-Fuhrman nuclear grade; 2: Metastasis at surgery; 3: N/A- Not available; 4: fold changes of the predominant POSTN band below 83kDa (T) versus it in ANK tissues (N); 5: Experiment Type: I – immunohistochemistry, IF-dual immunofluorescence, E – elisa, and W – western blot analysis.

Table 2: pRCC Patient Information

Patient	Age	Gender	Pathology	FG[1]	Metastasis[2]	Volume cm^3	POSTN Below 83kDa T/N[4]	POSTN at 83kDa T/N[4]	Experiment[5]
21	58	F	PRCC	3	N/A	25	1.902677	1.864947	W/IHC
28	56	M	PRCC	1	No	36.75	0.670739	1.771566	W/IHC
19	57	M	PRCC	3	N/A	96	1.016415	2.1721	W
50	64	M	PRCC	3	No	12.8	0.765276	0.300553	W
101	54	M	PRCC	3	No	58.32	0.693885	11.95337	W
103	74	M	PRCC	2	No	22.8	1.971115	1.889764	W
131	62	F	PRCC	2	No	22.5	0.393575	0.373541	W
135	59	M	PRCC	3	No	7.776	0.818074	0.222071	W
143	42	M	PRCC	3	No	121.5	0.704462	0.04811	W

1: FG-Fuhrman nuclear grade; 2: Metastasis at Surgery; 3: N/A-Not Available; 4: fold changes of the POSTN band below and at 83kDa in tumour (T) versus it in ANK tissues (N); 5: Experiment Type: I – immunohistochemistry, and W – western blot analysis.

Table 3: Metastatic ccRCC Patient Information

Patient #	Age	Gender	Pathology	Metastasis Location	Tumour Volume (cm^3)	Experiment Type
1	83	M	Clear Cell RCC	Bone	N/A	I
2	67	M	Clear Cell RCC	Lung	58.08	I
3	70	M	Clear Cell RCC	Lung	204.75	I,IF
4	61	M	Clear Cell RCC	Lymph Node	82.5	I,IF
5	57	F	Clear Cell RCC	Lung	544.5	I,IF
6	61	M	Clear Cell RCC	Colon	0.882	I
7	64	M	Clear Cell RCC	Back, subcut mass	170.52	I,IF
8	79	M	Clear Cell RCC	Urinary Bladder	0.1cm biopsy	I,IF
9	66	M	Clear Cell RCC	Lung	1.52	I,IF
10	47	M	Clear Cell RCC	Right Adrenal Gland	44.25	I,IF
11	62	F	Clear Cell RCC	Lung	0.3, 0.5cm biopsy	I
12	53	M	Clear Cell RCC	Lung	61.75	I
13	72	F	Clear Cell RCC	Perirenal Fat	0.1-0.5	I,IF
14	58	M	Clear Cell RCC	Lymph node	15	I
15	55	M	Clear Cell RCC	Lymph node	0.5cm biopsy	I
16	54	M	Clear Cell RCC	Adrenal	1.6, 1.1, 2cm biopsies	I,IF

Experiment Type: I – immunohistochemistry, and IF – dual immunofluorescence.

using Ultrospec 2100 pro spectrophotometer (Biochrom Ltd, Cambridge, England). Protein was stored in -80^{o}C for future applications.

3.4.2. Tissue Lysate Preparation

Tissue lysates were prepared from the non-tumour kidney and tumour tissues according to our published conditions (He *et al*., 2007). In brief, frozen renal cancer tissue and its corresponding adjacent normal renal tissue were retrieved from liquid nitrogen and then crushed under liquid nitrogen with a mortar and pestle in lysis buffer. Tissue lysates were stored in -80^{o}C until use.

3.5. Concentration of Periostin Protein in Media

At 80%-90% cell confluency, complete media was aspirated from cell culture plate and cells were washed with 1x sterile PBS, followed by addition of serum free media. Cells were incubated in a tissue culture incubator for 24 hours. 4 ml of media was then removed and centrifuged using an Amicon Ultra-4 centrifugal filter unit (Millipore, Billerica MA) at 3270 g for 15 minutes at 4^{o}C. The concentrated media was pipetted out of the filter and stored at -80 degrees until use.

3.6. Western Blot Analysis

50 µg of total lysate protein (for cell and tissue lysates) was diluted in 5xPSB (protein sample buffer, 0.1mM Tris pH 6.8, 5% SDS, 50% glycerol, 2% β-mercaptoethanol, 0.02% bromophenol blue and add ddH_2O to a final concentration of

1XPSB). The protein was denatured by boiling for three minutes at 100^{o}C in a heat block. The samples were separated on a 10% SDS-PAGE (sodium dodecyl sulphate polyacrylamide gel electrophoresis) gel with a 3% stacking gel at 50 mA in running buffer (20mM Tris-HCl, 192mM glycine, 1%SDS and ddH2O to a final concentration of 1x running buffer), followed by transfer in transfer buffer (25 mM Tris-HCl, 192 mM glycine, 20% methanol) onto Immobilon-P membranes (Millipore, Billerica MA) at 260 mA for 80 minutes. Membranes were blocked with 5% skim milk for one hour while shaking at 55 rpm and then washed with 1xTBST (Tris buffered saline + 0.1% Tween 20) at 150 rpm three times. Membranes were incubated at 4^{o}C over night with the indicated antibodies prepared in 5% bovine serum albumin solution in 1x TBST. The appropriate secondary antibodies were prepared in 5% skim milk and incubated for an hour at 55rpm. The membranes were then washed with 1xTBST three times for 10 minutes each. Signals were detected using an ECL Western Blotting Kit (Amersham, Pittsburg PA). Excess ECL solution was absorbed using a paper towel before exposure onto Kodak X-OMAT X ray film. Primary antibodies and concentrations used were: anti-periostin 1:1000 (Abcam, Cambridge MA), anti-actin 1:1000 (Santa Cruz, Santa Cruz CA), anti-phospho AKT 1:500 (Cell Signaling, Danvers MA), anti-AKT 1:1000 (Santa Cruz, Santa Cruz CA), anti-phospho GSK 1:1000 (Cell Signaling, Danvers MA), anti-GSK 1:1000 (Santa Cruz, Santa Cruz CA), anti-phospho P70S6K 1:1000 (Cell Signaling, Danvers MA) and anti P70S6K 1:1000 (Cell Signaling, Danvers MA). Western blot images were analyzed using imageJ software (National Institute of Health, USA). The average POSTN fold change was calculated by first normalizing the POSTN band to their respective actin band for both ccRCC and ANK for each patient (ex: ccRCC POSTN value/ccRCC Actin value) . Then fold change was calculated using the formula: Avg POSTN fold change = Avg POSTN value in ccRCC/ avg POSTN value in ANK

3.7. Generation of Xenograft Tumours

This experiment was conducted by previous students and I utilized the xenograft tissues for my IHC analysis. A498 cells were resuspended into a MEM/Matrigel mixture (1:1 volume). $3x10^6$ cells in 0.1 ml were subcutaneously implanted into flanks of 8 weeks old NOD/SCID mice. Tumour growth was measured weekly using a caliper. Tumour volume was determined using the standard formula: $L \times W^2 \times 0.52$, where L and W are the longest and shortest diameters, respectively. The presence of each xenograft tumour was confirmed by H & E staining. All animal work was carried out according to experimental protocols approved by the McMaster University Animal Research Ethics Board.

3.8. IHC and Dual IF

3.8.1 IHC

IHC was performed on 9 paraffin-embedded and serially-cut primary ccRCC tissues, 2 pRCCs, 16 metastatic ccRCC tissues obtained from St. Joseph's Hospital, Hamilton, Canada. Available A498 cell-derived xenograft tumours from NOD/SCID mice were also IHC analysed. Briefly, slides were deparaffinised in three changes of xylene for 10 minutes each and cleared in ethanol series 2x 2 min in 100% and 2 x 2min in 70% ethanol. The endogenous peroxidise was then quenched using 3% H_2O_2 in water for 10 minutes. The antigen retrieval was conducted by heat-treating the slides for 30 minutes in sodium citrate buffer (pH = 6.0) in a food steamer. Primary antibodies specific for POSTN 1:1000 and factor VIII 1:250 were incubated with the sections overnight at 4°C. Negative controls were incubated with a non-specific anti-rabbit IgG. Biotinylated goat anti-rabbit IgG secondary antibody and Vector ABC reagent (Vector Laboratories, Burlingame CA) were subsequently added according to the manufacturer's instructions. Washes were performed with 1x PBS. The chromogen reaction was carried out with diaminobenzidine (DAB), and counterstaining was done using haematoxylin. Haematoxylin and eosin (H&E) staining was carried out using a standard protocol. The slides were dehydrated in 70% ethanol, 100% ethanol and then two changes of xylenes and were subsequently covered with a cover slip using cytoseal mounting medium (Richard Allan Scientific, Kalamazoo, MI).

3.8.2. Dual IF

Paraffin embedded sections were deparaffinised in three changes of xylene for 10 minutes each, 2 changes of 100% ethanol 1 min each, then 2 changes of 70% ethanol one minute each. The slides were then washed in distilled water three times. Heat-induced antigen retrieval was conducted in a food steamer for 25 minutes then the slides were washed in 1x PBS buffer twice. Tissue was blocked with 5% normal donkey serum in 1x PBS for one hour at room temperature. The slides were washed again with PBS and then incubated with the cocktail of primary antibodies over night in a 4^{o}C room. The antibodies used were: anti POSTN, anti alpha smooth muscle actin (SMA), anti factor

VIII and anti fibronectin. Slides were rinsed with 1xPBS and subsequently incubated with the secondary antibody cocktail made in PBS in a 1:100 dilution. Slides were washed in PBS, distilled water, followed by mounting with Vectashield mount containing DAPI. The tissues were visualized using a fluorescent microscope under the fluorescence filters FITC, Cyb5 and DAPI.

3.9. Competition of Periostin Antibody with Recombinant Periostin Protein

Multiple dilutions of the POSTN antibody were prepared (1:1000, 1:1500, 1:2000, 1:5000, 1:8000) and probed on a western blot of a ccRCC patient's tumour lysate. The dilution 1:5000 was selected because it clearly displayed the POSTN band with the least amount of background stain. 10 µg/ml of recombinant human POSTN protein (R&D systems Minneaapolis MN) was incubated with 1:5000 diluted antibody (1µg/µl) in a 5ml volume for two hours on ice. The membrane was incubated on a shaker at $4^{o}C$ overnight with the antibody plus recombinant protein solution. A separate membrane with the same patient's protein lysate was incubated with POSTN antibody as a positive control. This procedure was repeated for IHC (Fig 7).

3.10. ELISA Analysis of Serum Periostin

A sandwich ELISA protocol was followed. A 96 well microtiter plate was utilized for this procedure. The plate was coated with a capture antibody, polyclonal goat anti-POSTN antibody (Santa Cruz) at 2 µg/µl in carbonate coating buffer (71 mM $NaHCO_3$ and 28.6 mM Na_2CO_3) pH 7.4. The plate was incubated over night in $4^{o}C$, followed by rinse with 200 µl of PBS-T (PBS + 0.05% Tween 20) twice. The wells were blocked with 200 µl blocking buffer (5% non fat milk in PBS) for two hours at room temperature. The plate was rinsed before addition of samples (100 µl) for two hours at room temperature, which was followed by washing the wells with PBS-T and incubation with the detection antibody [polyclonal anti-POSTN rabbit IgG (AbCam)] for one hour at room temperature. The plate was washed four times with PBS-T and then incubated with 80 µl of secondary antibody diluted in blocking buffer for 1 hour at room temperature. Finally 3,3′,5,5′-Tetramethylbenzidine (TMB) Substrate (Sigma Aldrich, St.Louis MO) was added to the wells and the reaction was stopped by adding 2N HCL. Absorbance was recorded on an ELISA reader at 450 nm.

3.11. Generation of Stable Cell Lines

3.11.1. Sub Cloning Periostin

The POSTN cDNA was inserted into the C-FLAG pcDNA plasmid. pcDNA 3.0 plasmid was purchased from Clontech (Mountain View, CA). Primers were designed to add HindIII and Xho sites to the cDNA during polymerase chain reaction (PCR). The designed PCR primers were: HindIII 5' CCC AAG CTT ATG ATT CCC TTT TTA CCC ATG T, and Xho 5'CCA CTC GAG CTG AGA ACG ACC TTC CCT TAA. 100 ng of cDNA, 20 pM of each primer, 200 µM of dNTP, 0.4 µl of pfu , 5 µl of 10x buffer and sterile water were prepared in a 50 µl PCR reaction. After conducting PCR, the DNA was run on an agarose gel and the appropriate size band for POSTN was retrieved using gel extraction. POSTN cDNA was digested sequentially with the HindIII and Xho restriction enzymes (Invitrogen, Carlsbald CA), ethanol precipitated and ligated together using a DNA rapid ligation kit (Roche, Mississauga, ON). Following the ligation of the POSTN cDNA into the C-FLAG pcDNA vector backbone, bacteria was transformed with the plasmids (vector or vector + insert). Colonies from the vector plus insert plate were screened and positive clones were sequenced. 293T cells were transiently trasfected with either the POSTN plasmid or pcDNA-C FLAG control, followed by the examination of ectopic POSTN by western blot. Next, the POSTN gene was digested out of the pcDNA plasmid with the C-FLAG attached. The POSTN cDNA was then cloned into a retroviral pLPCX vector.

3.11.2. Stable Cell Line Production

A stable cell line was generated using NIH3T3 fibroblast cells. 10 µg of pVPack-VSV-G, and 10 µg of pVPack-GP [Agilent Technologies (Mississauga, ON)] plus 10 µg of the retroviral vector (POSTN in PLPCX or PLPCX EV control) were used for a calcium phosphate transfection into 293T cells. The calcium phosphate transfection cocktail included 50 µL of 2.5M $CaCl_2$, H_2O and the required vectors for a total volume of 500 µl in a 13 ml tube. In between the addition of each component of the cocktail the tube was gently vortexed to mix the solution. Subsequently, another tube with 500 µl of 2x HeBS (HeBS, 0.28 M NaCl, 0.05 M hepes, 1.5 mM $Na_2HPO_4 \cdot 7\ H_2O$, pH 7.1) was gently vortexed as the solution from the first tube was added drop wise using a glass pipette, followed by 30 seconds of vortexing. This solution was incubated at room temperature for 20 minutes. Next, using a Pasteur pipette the transfection solution was mixed several times and added drop wise to the entire plate of 293T cells, the plate was mixed in a figure eight configuration to allow for proper distribution of calcium and DNA precipitate. The plate was incubated for 10 hours at 37^oC and 5% CO2. Media was then changed for fresh complete DMEM media. Cells were incubated for another 48 hours. At this point, the supernatant containing virus particles was obtained and filtered through a 0.45 μm filter, 3 mL of supernatant was incubated with NIH3T3 cells, which were seeded the night before infection. The NIH3T3 cells with the virus supernatant was swirled in the tissue culture plate every 20 minutes for two hours. Virus media was then replaced with fresh media and incubated for another 24-48 hours at which point the cells were selected by the addition of 1μg/ml of puromycin.

3.12. Immunoprecipitation (IP)

IP is a technique used to pull down a protein from a lysate using a specific antibody. In this method, 20µl of agarose beads were resuspended in 1ml Co-IP buffer (50mM Tris-Cl ph7.5, 150mM NaCl, 1mM EDTA, 0.1% Triton X-100) followed by centrifugation of the beads at 2000rpm for five minutes in a 4^oC centrifuge. The supernatant was then aspirated out and the beads were resuspended in 1ml of Co-IP buffer and this wash step was repeated three times. After which, the beads were resuspended back into the necessary volume (1:1 dilution). Next, the Co-IP cocktail was prepared in a 1.5ml centrifuge tube: 900µl of Co-IP buffer, 20µl of protein G agarose beads, 1-2mg of protein, 1µg of antibody; followed by placement of this tube on a nurator in the 4^oC room overnight. The reaction was centrifuged at 2000 rmp at 4^oC for five minutes, followed by washing the beads with 800ul of Co-IP buffer eight times. The resulting pellet was resuspended in 2X protein sample buffer and boiled for 5 minutes for analysis by western blot. The 2xPSB and boiling of the sample allowed the protein to dissociate from the beads and the supernatant was subsequently analyzed by western blot.

3.13. Colony Formation Assay

NIH3T3 EV and POSTN cells were seeded at 100, 500, or 1000 cells per well, followed by culture in DMEM media in the presence of 1 µg/ml puromyocin for approximately two weeks until the colonies being clearly visible. Media was changed every 3 days. At the end of the two weeks, media was aspirated and the plate was washed twice with 1xPBS. The cells were then fixed with fixing solution (2% formaldehyde and 0.2% glutaraldehyde in PBS) for 20 minutes, washed with PBS and stained for 20 minutes with 0.3% crystal violet. Excess staining including background stain was reduced by dipping the plates into water multiple times. This experiment was repeated 3 times.

3.14. Co-culture Experiment

A498 or 786-0 ccRCC cells and NIH3T3 fibroblast cells were co-cultured in a 1:1 raio. The control plates were A498, NIH3T3 and 786-O cells grown separately for the same duration of time. At 80% confluency RNA was extracted for qRT-pCR or cell lysates were prepared for protein analysis.

3.15. RNA Analysis

3.15.1. RNA Extraction

RNA was extracted from cells using TRIzol solution according to the manufacturer's instructions. In brief, 3ml of TRIzol was added to the cell culture plate and pippetted several times. The solution was incubated for five minutes at room temperature, followed by adding 0.2ml of chloroform per 1ml of TRIzol. Tubes were shaken vigorously and incubated again for three minutes at room temperature, followed by centrifugation at 11,000rpm for 15minutes at 4^{o} C. RNA in the aqueous phase was removed and 0.5ml isopropyl alcohol was added per ml of TRIzol. This solution was incubated for 10 minutes at room temperature and centrifuged again at 11,000rpm for 10 minutes. The RNA pellet was washed with 75% ethanol in DEPC water and the dried pellet was dissolved in RNase free water by incubation for 10 minutes at 55^{o}C. The resulting RNA was stored at -80^{o}C until use.

3.15.2. Real Time PCR

Two micrograms of RNA was converted to cDNA. A mixture of dNTP, random and oligo primers, RNase out, the RNA and DEPC water were mixed and placed in the PCR machine at 65^{o}C for six minutes. To the mixture 5x strand buffer, DTT, RNase out and superscript III were added on ice, followed by incubation at 25^{o}C for 11 minutes for one cycle, then 50^{o}C for one hour. Final extension proceeded at 70^{o}C for 15 minutes and the reaction was maintained at 4^{o}C until sample was removed. The cDNA was diluted 1:4 in nuclease free water, which was used to amplify murine POSTN and murine GAPDH, or human POSTN and human actin by real time PCR using specific primers (Table 4).

The real time reaction mixture also included SYBR green. Each sample was run with a triplicate.

Table 4: Semi-Quantitative Real Time PCR Primers

Gene	Primer sequence	Reference
Human periostin forward	5'-TGC CCA GCA GTT TTG CCC AT-3’	Tilman et al, 2007
Human periostin reverse	5'-CGT TGC TCT CCA AAC CTC TA-3’	Tilman et al, 2007
Murine periostin forward	5’- TGC TGC CCT GGC TAT ATG AG -3’	Nishiyama et al, 2011
Murine periostin reverse	5’-GTA GTG GCT CCC ACA ATG CC-3’	Nishiyama et al, 2011
β-actin (human) forward	5’- ACC GAG CGC GGC TAC AG-3	Tang Lab
β-actin reverse	5’- CTT AAT GTC ACG CAC GAT TTC C-3’	Tang Lab
GAPDH (murine) forward	5’- TCA CCA TCT TCC AGG AG- 3’	Tang Lab
GAPDH reverse	5’- GCA TTG CTG ACA ATC TTG AGT GAG-3’	Tang Lab

3.16. Cell Attachment and Growth Assay

Petri dishes were coated with either 10 µg of recombinant POSTN in PBS or recombinant glutathione S-transferase (GST) in PBS as a control. These plates were incubated over night at 4^0C, washed with PBS, blocked with 1 % BSA for one hour., and washed again. A498 cells ($4x10^4$) were then seeded in 2% FBS containing MEM media. After 45 minutes non adherent cells were removed and attached cells were cultured in MEM supplemented with 2% FBS for 5 hours to enhance attachment. The plates were then washed several times with PBS, followed by staining with 0.5% crystal violet. To assay the attachment properties of NIH3T3 EV and POSTN cells, uncoated petri dishes were used. The rest of conditions remained the same. For the cell proliferation assay the cells were allowed to adhere and then cultured for 48 hours before staining with 0.5% crystal violet.

3.17. Wound Healing Assay

A 6 well plate was seeded with 50,000 NIH3T3 POSTN and EV cells and cultured for 2 days in a 37^{o}C incubator until cells were 100% confluent. A wound was then introduced by using a 1ml blue pipette tip to create a vertical scratch through the cells. The media was then aspirated to remove the cells that had been scraped off. This was followed by the addition of 2ml of DMEM media to each well. Images of the vertical scratch (wound) were taken at three different locations, top, middle and bottom of the line. Images were taken at 2.5x and 5x magnification at 0, 4 hours, 8 hours and 24 hours.

IV. RESULTS

4.1. Robust Upregulation of Periostin in ccRCC

In an effort to examine POSTN expression in RCC, I have conducted western blot analysis on 27 human ccRCC and 9 pRCC (Tables 1, 2) along with ccRCC cell lines 786-O, A498, ACHN and 1933 (Fig 4A). Of the 27 ccRCC tissues (eight stage one, 10 stage two, eight stage three and one stage four), POSTN was overexpressed in ccRCC compared to ANK in 26 patients except for one case. Western blot results were quantified using imageJ software. The observation that ANK tissues express low or undetectable levels of POSTN is consistent with POSTN being primarily expressed in the bone, teeth and heart (Horiuchi *et al*., 1999; Ruan *et al*., 2009). The levels of POSTN upregulation also fluctuate amongst tumours (Fig 4C). This fluctuation was not caused by a variation in protein degradation during lysate preparation since comparable amount of actin was readily detected in all tissues (Fig 4A). Despite this variation, it is clear that the majority of ccRCCs examined display elevated POSTN expression (Fig 4A, Table 1). The levels of POSTN protein were significantly higher in ccRCC in comparison to ANK (Fig 4B) (*$p < 0.05$).

We next investigated POSTN expression in pRCC using western blot analysis (Figure 4D, Table 2). We noted marked variability between the 9 pRCC samples with bands appearing both below and at the 83kDa mark. These bands have been individually quantified using Image J. For the POSTN bands below 83kDa, six pRCC samples had a higher level of POSTN in the adjacent kidney tissue, while three samples exhibited a higher level of POSTN in the pRCC.

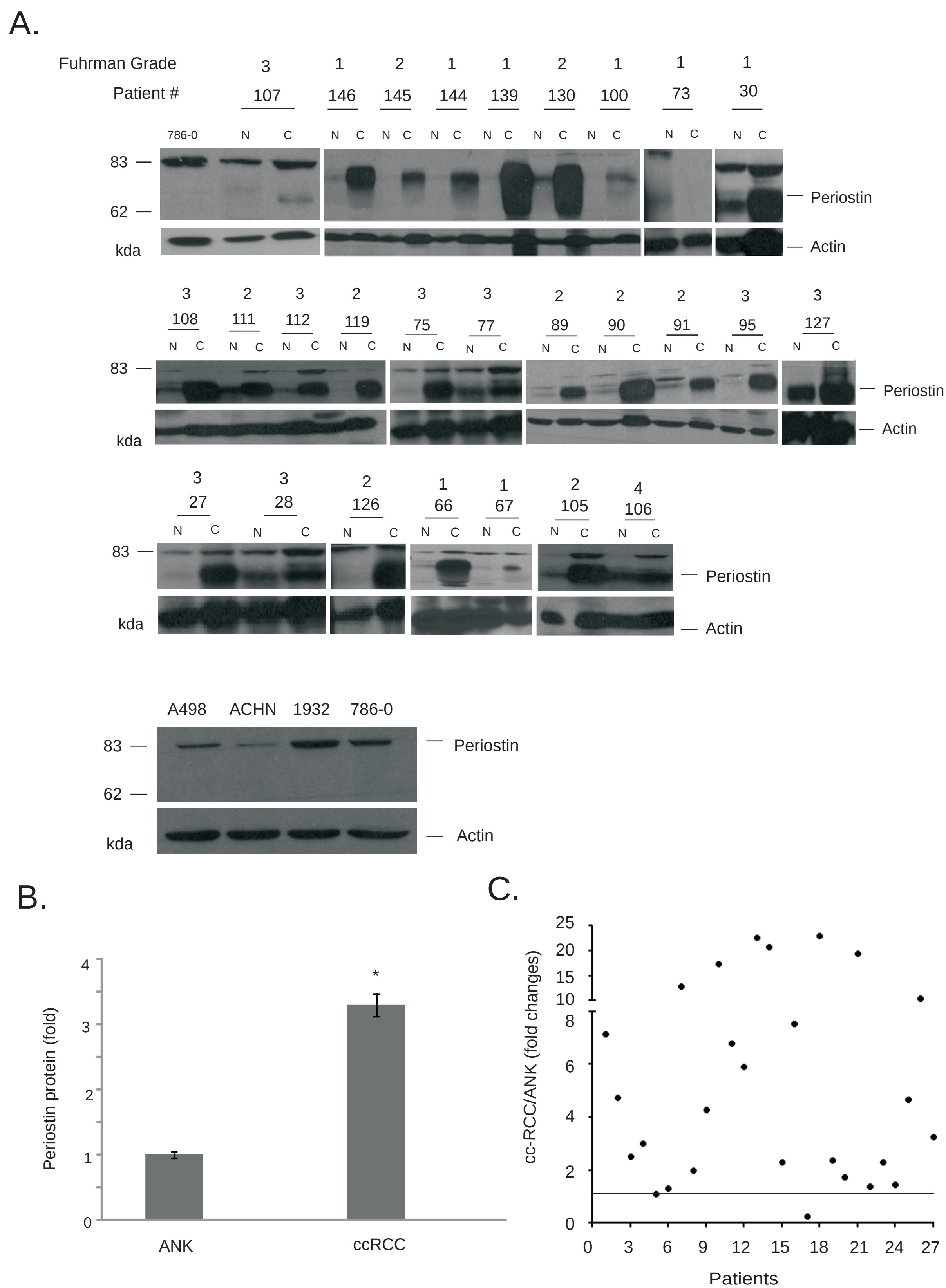
A.
Fuhrman Grade
Patient #
786-0
N C
83
62
kda
Periosstin
Actin
A498 ACHN 1932 786-0
B.
Periostin protein (fold)
ANK
ccRCC
*
C.
cc-RCC/ANK (fold changes)
Patients

D.

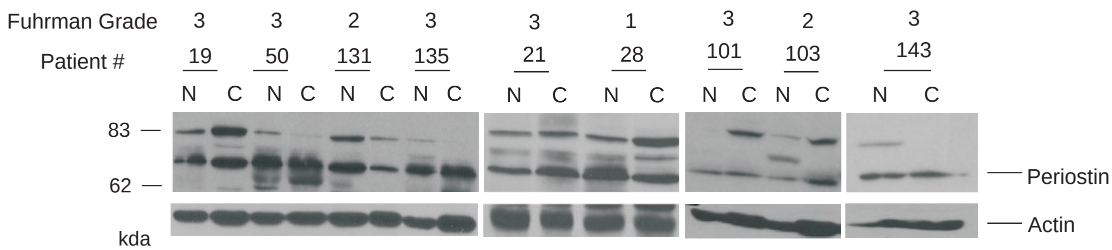

Figure 4. Up regulation of periostin in ccRCC. **A)** Western blot analysis of periostin in the lysates of ccRCC patients and indicated ccRCC cell lines (786-0, A498, ACHN, and 1932). Tumour grade along with patient number are indicated. N: adjacent non-tumour kidney (ANK) tissues; C: tumour tissues. Robust periostin upregulation detected between 62 and 83kDa in tumour tissues in comparison to ANK. **B)**Western blot analysis was performed on 27 ccRCC patients using the imageJ software. Periostin in ANK and ccRCC were normalized to their respective actin for all patients analyzed (See Table 1 for patients subject to wetsern blot analysis). The levels of periostin were expressed as fold changes to the POSTN levels present in ANK tissues (refer to Materials & Methods: western blot analysis for details on calculation) * $p < 0.05$ in comparison to ANK determined by 2-tailed Student's t test. **C)** Periostin expression in ccRCC patients were expressed as fold changes to the levels in the respective ANK. The distribution of these changes is graphed. The horizontal line represents 1 fold or no change and the dots below or above the lines are down regulated or up regulated. **D)** Western blot analysis of periostin in ANK (N) and the respective pRCC (C) (See Table 2 for patient details).

For the bands at 83kDa, five out of the nine samples had a higher level of POSTN in the pRCC when compared to ANK. To determine whether these bands represent the POSTN protein, I conducted an antibody blocking experiment using recombinant POSTN protein (Fig 7D). As both bands were apparently blocked by recombinant POSTN, these may represent different isoforms of POSTN. Thus, evidence here does not support an alteration of POSTN in pRCC compared to the adjacent non-tumour kidney tissues. Collectively, the above results revealed a robust upregulation of the POSTN in ccRCC determined through the ratio of ccRCC/ANK values after imageJ analysis.

4.2. ccRCC is Associated with Predominant Stromal Persiostin

4.2.1. Periostin Expression in Organ-Confined ccRCC

ccRCC is widely regarded to originate from the proximal tubular epithelial cells (Newman *et al*.,1997; Maher *et al*., 1997; Choyke *et al*., 2003). To examine the tissue distribution of POSTN in ccRCC, available tumour tissues from nine different patients were utilized for IHC. These patients exhibited stage 1, 2 , 3 ccRCC. In ANK tissues, POSTN was detected in the proximal tubular epithelial cells but not inside of the glomerulus, (confirmed through consultation with nephrologist Dr.Margetts). This expression pattern was observed in all ANK tissues analyzed (Fig 5). The POSTN levels in ANK tissue was overall weak, which is in line with the reported tissue distribution of POSTN. POSTN is present in certain normal adult tissues such as aorta, stomach, lower gastrointestinal tract, placenta, uterus and breast but not the kidney (Gillan *et al*., 2002).

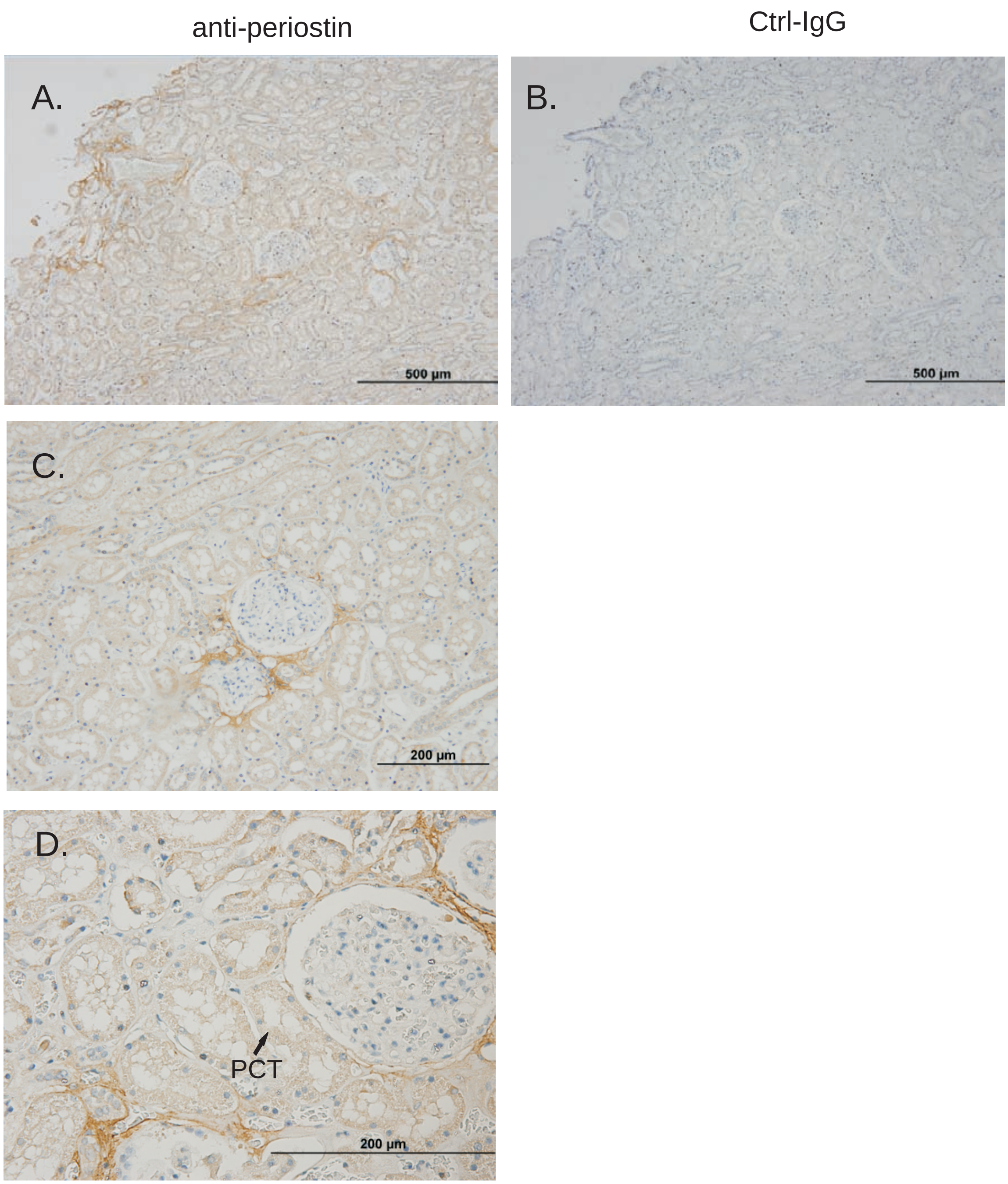

Figure 5. IHC analysis for anti-periostin antibody in adjacent non-tumour kidney tissue (ANK) of a ccRCC patient. Periostin detected mainly in the proximal tubular epithelial cells. Images taken under increasing magnifications to show tissue distrubution of periostin. **A)** Periostin detection under 10x magnification. **B)** Negative control (Ctrl) using non specific anti-rabbit IgG in place of periostin antibody. **C)** Periostin detection under 20x magnification. **D)**Periostin detection under 63x magnification, image displays the tubular cells and the glomerulus of the nephron. Scale bars represent 500 µM and 200 µM. Arrow points to proximal convoluted tubules (PCT).

POSTN has been reported to be a secreted cell adhesion protein and induce ovarian cancer cell motility (Gillan *et al*., 2002), suggesting that its tumour promoting functions can be attributable to the secreted form of POSTN. In support of this concept, we demonstrated that POSTN existed predominantly as a stromal protein in ccRCC (confirmed by pathologist Dr. Cutz) (Fig 6A). In comparison to the ANK tissues, the intensity of the POSTN expression in ccRCC was significantly higher (Fig 6A), which confirms our western blot results (Fig 4). POSTN tissue distribution in pRCC was also examined. While some stromal POSTN was detected, POSTN largely existed in the cancerous cell of pRCC tissues (Fig 6B). To confirm the IHC results for ccRCC and pRCC tissues being specific for POSTN, a POSTN blocking experiment was conducted (Fig 7). The presence of recombinant POSTN protein significantly reduced anti-POSTN antibody's ability to recognize ccRCC-associated POSTN (Fig 7B). Taken together, the above observations reveal that POSTN is expressed in the stroma of ccRCC tissues.

4.2.2. POSTN Expression in Metastatic ccRCC

We demonstrated that POSTN is predominantly expressed in the stroma of organ confined ccRCC. Next, I was interested in investigating the POSTN expression pattern before and after ccRCC metastasis to determine if there exists a correlation between POSTN expression and ccRCC metastases. For this purpose, I have conducted IHC analysis to detect POSTN expression in six primary ccRCCs and their metastatic counterparts. IHC for each primary ccRCC and its metastatic counterpart was conducted simultaneously. The metastases sites for these six cases include lung, lymph node,

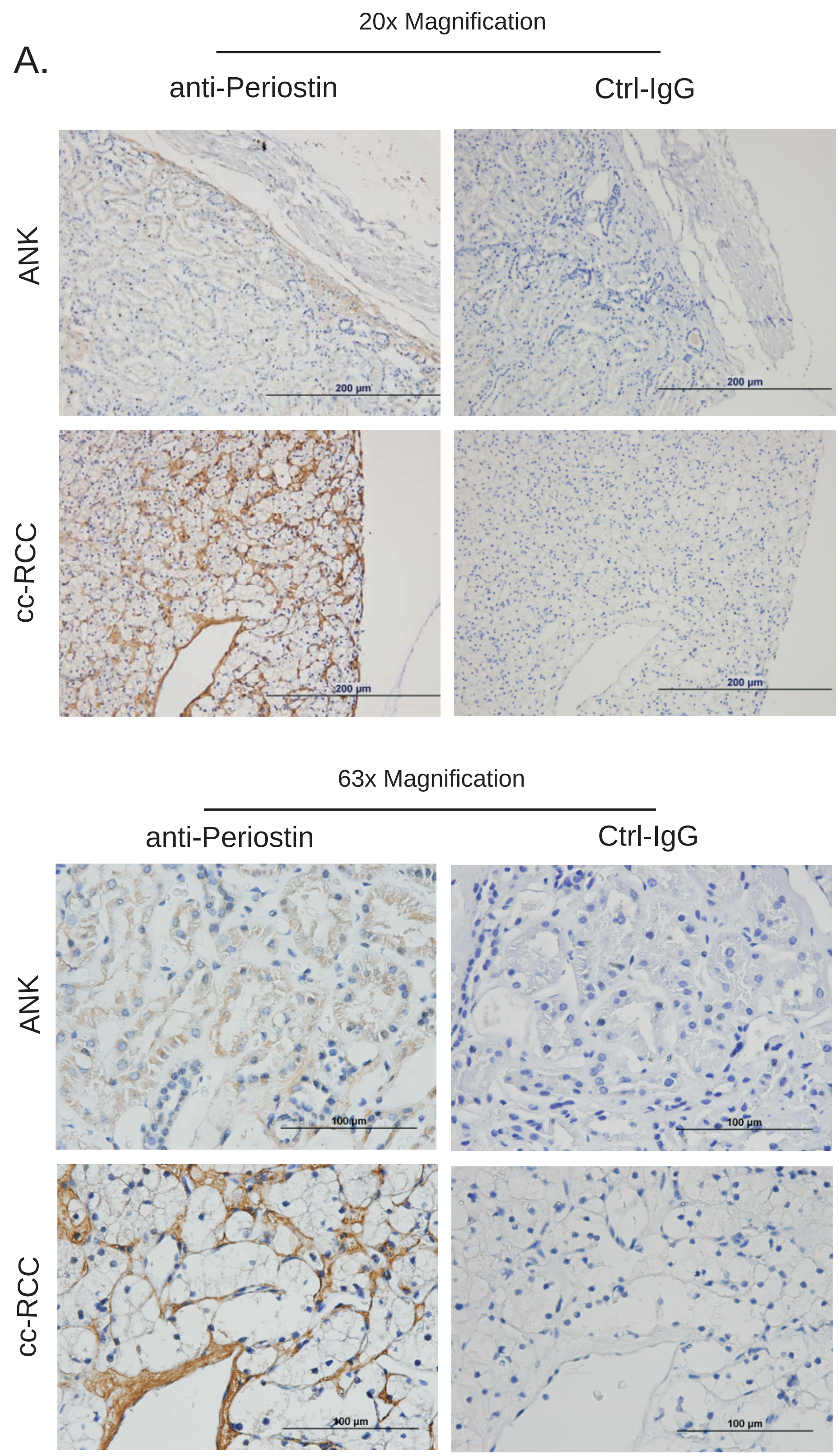
20x Magnification
A.
anti-Periostin
Ctrl-IgG
ANK
cc-RCC
200 µm
200 µm
200 µm
200 µm
63x Magnification
anti-Periostin
Ctrl-IgG
ANK
cc-RCC
100 µm
100 µm
100 µm
100 µm

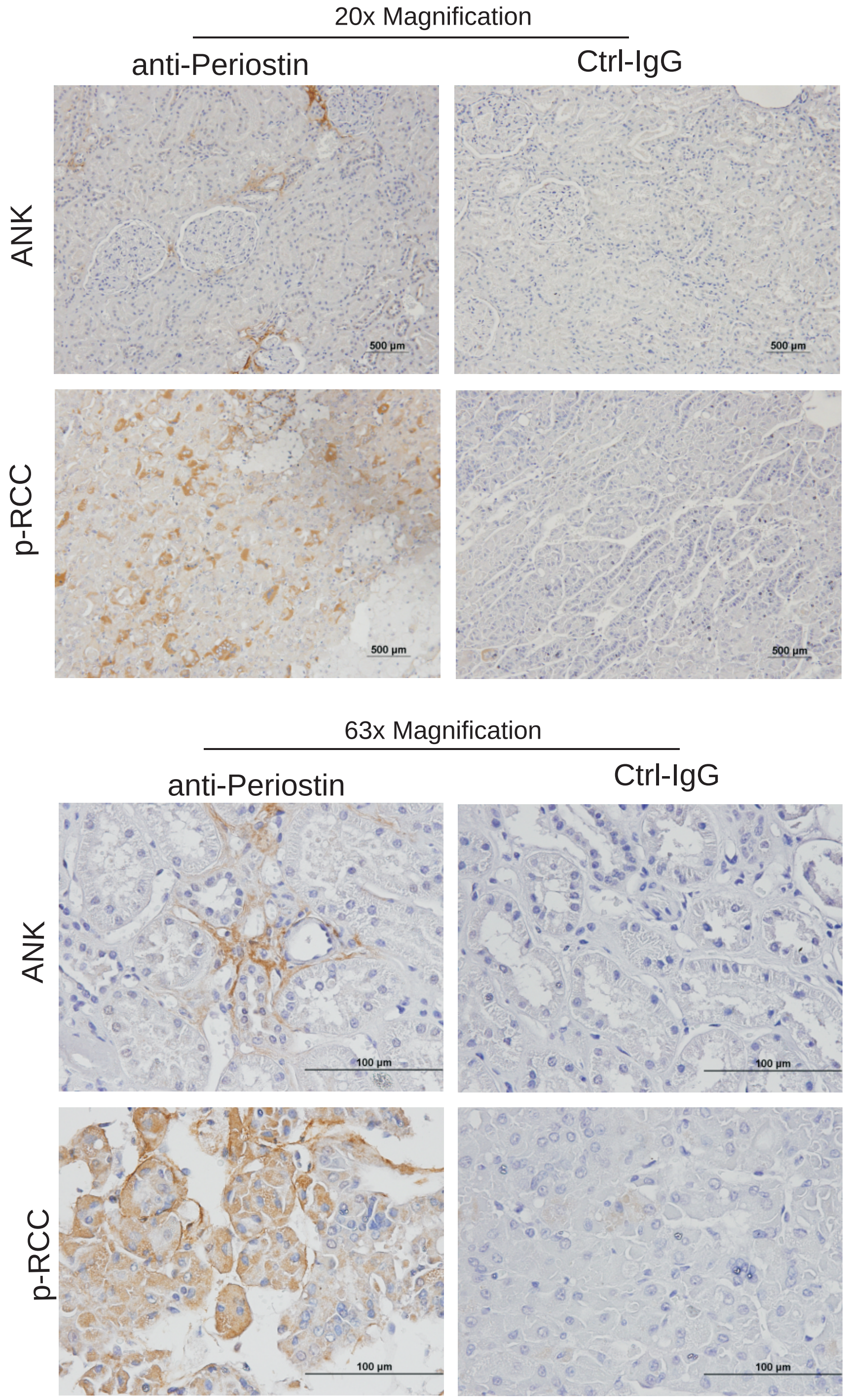

Figure 6. IHC using POSTN antibody was performed on ccRCC (**A**) or pRCC (**B**). **A)** Expression of POSTN was abundant in the stroma of ccRCC, where as POSTN expression was detected in the tubular epithelial cells of ANK tissues. Panel of images on the bottom were taken at a higher magnification (60x) for the purpose of clarity of POSTN localization. (**B**) POSTN was detected inside the papillary tumour epithelial cells of pRCC. In contrast, POSTN was expressed predominantly in the extracellular regions for the ANK tissue. Panel of images on the top were taken at 20x magnification and panel of images on the bottom were taken at 60x magnification. Scale bars represent 200 µm for the top panels, and 100 µm for the bottom panels, respectively.

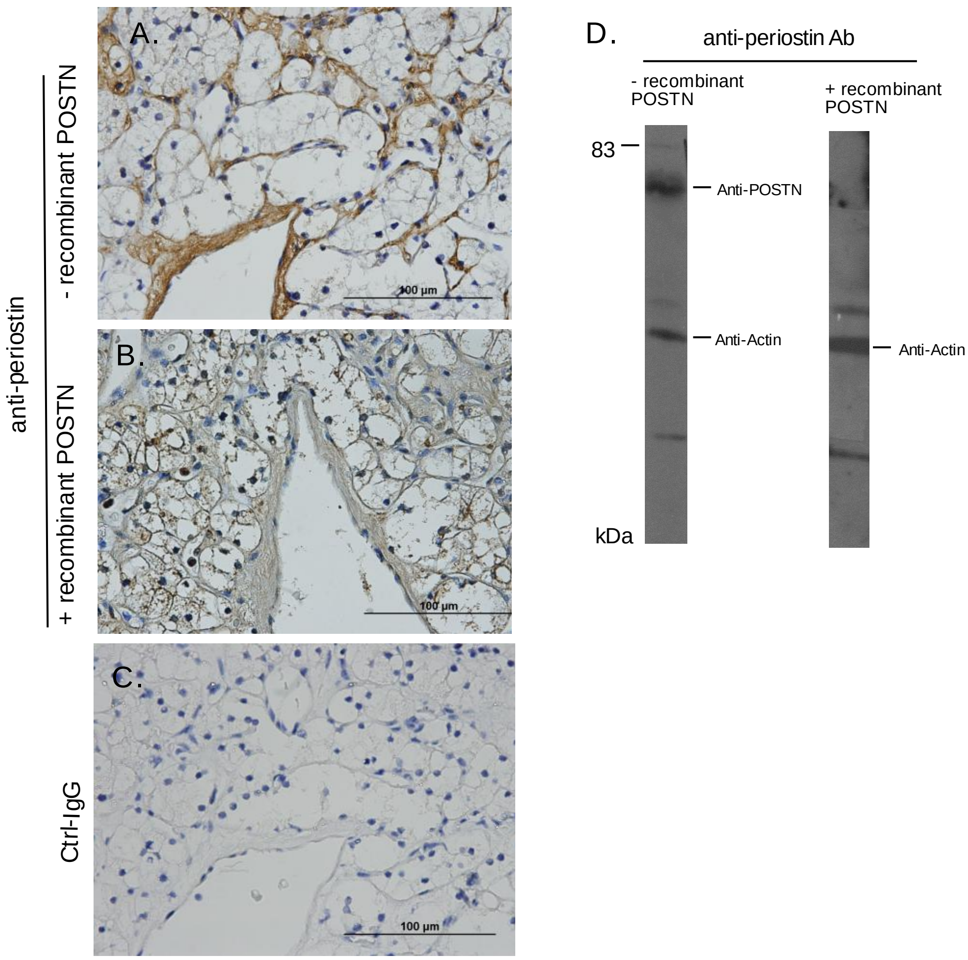

Figure 7. Anti-periostin antibody specifically recognizes periostin protein. **A)** IHC analysis conducted on ccRCC tissue for periostin protein. **B)** IHC analysis of POSTN in the presence of recombinant periostin. The source of the recombinant human periostin was murine myeloma cell line (R&D systems, Minneapolis MN). 10ug/ml of the protein was used and a 5ml solution of antibody and recombinant protein was made. The antibody dilution selected was 1:5000 periostin in TBST. **C)** Cntrl-igG. Images captured at 63x magnification. **D)** Western blot analysis of ccRCC patient's tumour tissue without the presence of recombinant POSTN and with recombinant POSTN. Actin was also detected. POSTN expression below 83kDa and the band at 83kDa were both eliminated due to the presence of recombinant POSTN with the POSTN antibody.

perirenal fat and adrenal gland. In both primary and metastatic tumours, the most intensive POSTN expression was localized in the stromal region of the tumour -non-tumour boundary (Fig 8A). Some of the metastatic tumours displayed POSTN expression spanning a greater area in the tumour-non-tumour boundary compared to the primary tumour. This was established through analysis utilizing a light microscope comparing the primary tumour with its respective metastatic tumour (Fig 8 A, B).

We wanted to verify whether stromal expression of POSTN in metastatic ccRCC tissues was a consistent occurrence. To perform IHC analysis for POSTN in a larger cohort of metastatic ccRCC cases, we retrospectively searched for metastatic ccRCC cases from several thousand cases of patients who had tissue resection in the Hamilton HealthCare System during the past several years. We identified 16 clinically confirmed metastasized ccRCC tumours. This included six lung metastases, one case for bone metastasis, three lymph node, two adrenal, one colon, one urinary bladder, one back subcutaneous and one perirenal fat (Table 3). Prominent stromal POSTN was clearly detected in all metastatic ccRCC cases, regardless of the site of metastases (Fig 9). In the lung metastases, while POSTN was clearly detected in the intra-tumour stroma, in the stroma situated between tumour and non-tumour tissues POSTN was most abundantly expressed (Fig 8, Fig 9). Collectively, we have demonstrated that metastatic ccRCC tumours are associated with abundant stromal POSTN. In addition, a pattern emerged during the metastatic tumour analysis where POSTN was often expressed in the stroma adjacent to the tumour boundary and spreading inwards into the tumour mass (Fig 10).

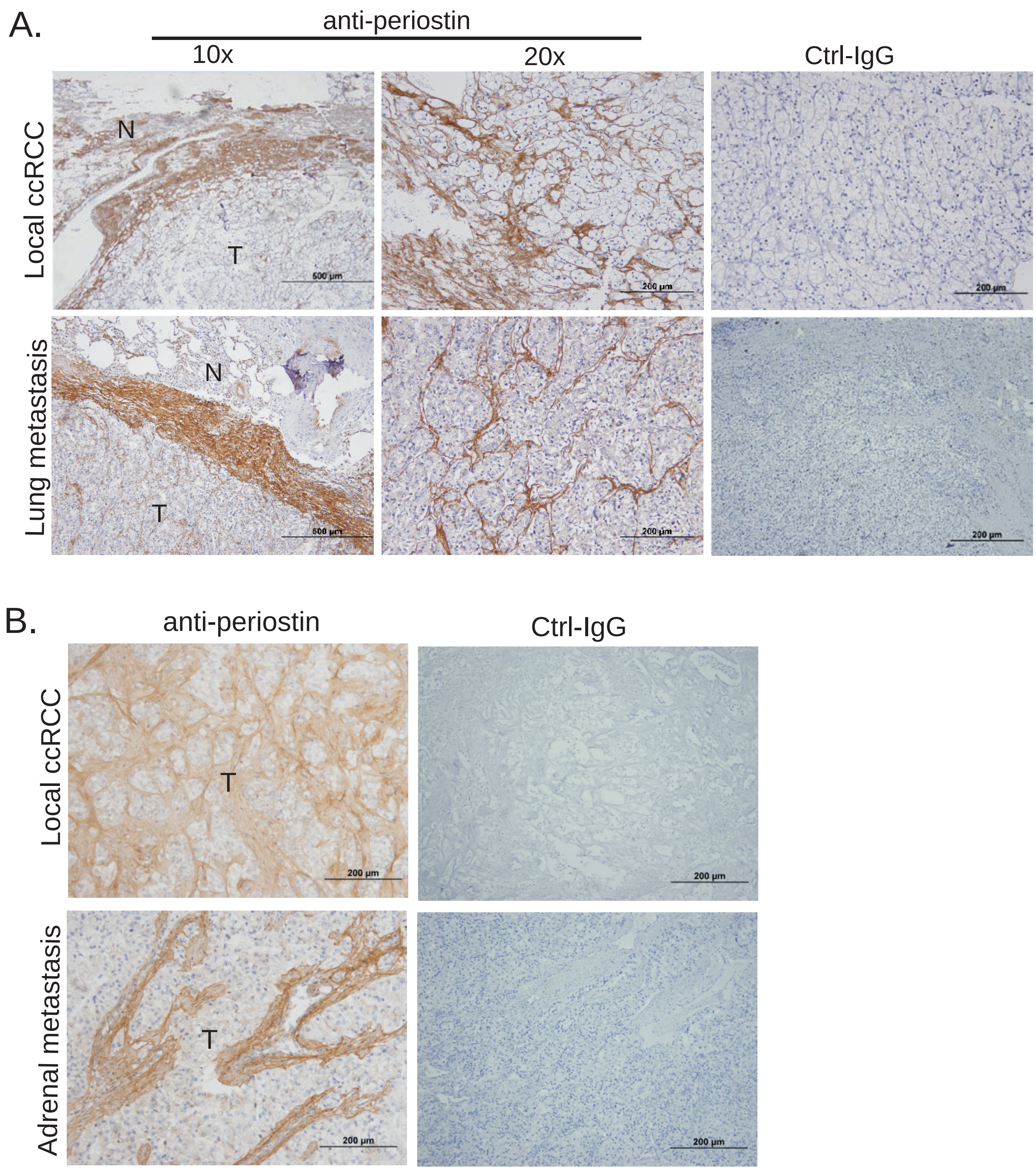

Figure 8. IHC analysis of POSTN in two cases of local and metastasized ccRCC. **A)** POSTN expression in the boundary between tumour (T) and non tumour (N) regions for the primary ccRCC and its corresponding lung metastases. Lung metastases displays POSTN expression spanning a greater area in the boundary when compared to primary ccRCC. The center panel represents images taken at higher magnification to illustrate details of POSTN expression in intra-tumour regions. Right most panel represents non specific anti-rabbit control (Ctrl) IgG. **B)** Primary and adrenal metastasized ccRCC tumours with control IgG. Intra-tumour regions illustrating POSTN expression.

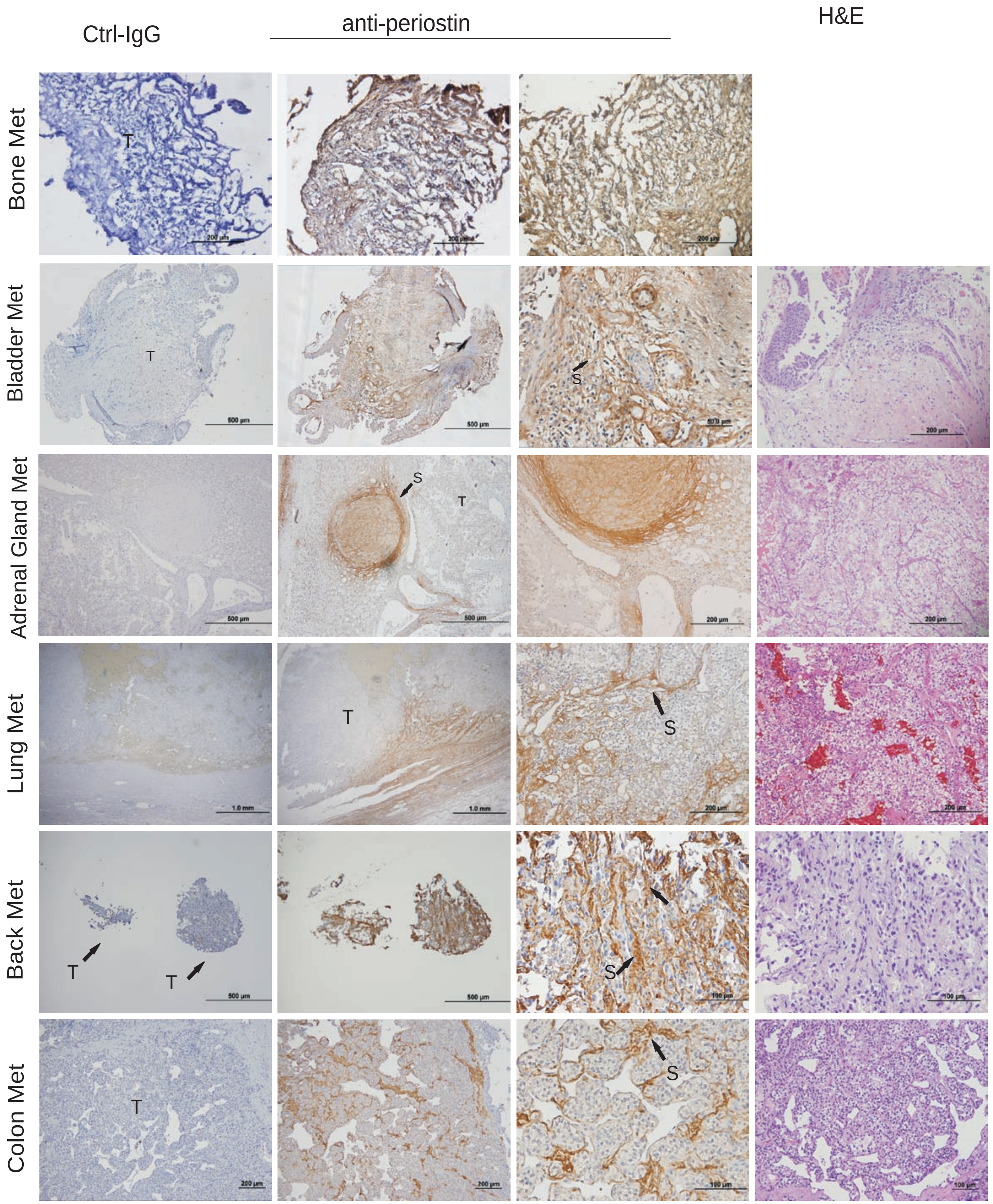

Figure 9: IHC analysis of POSTN expression in metastasized ccRCC to various secondary organs. Column 1 is the control Ctrl-IgG, columns 2 and 3 are images taken at low and high magnification to display the intra tumour expression of periostin. Column 4 is H&E stain for available tissues. T: Tumour. S: Stroma. Black arrows point to either tumour mass or stromal component.

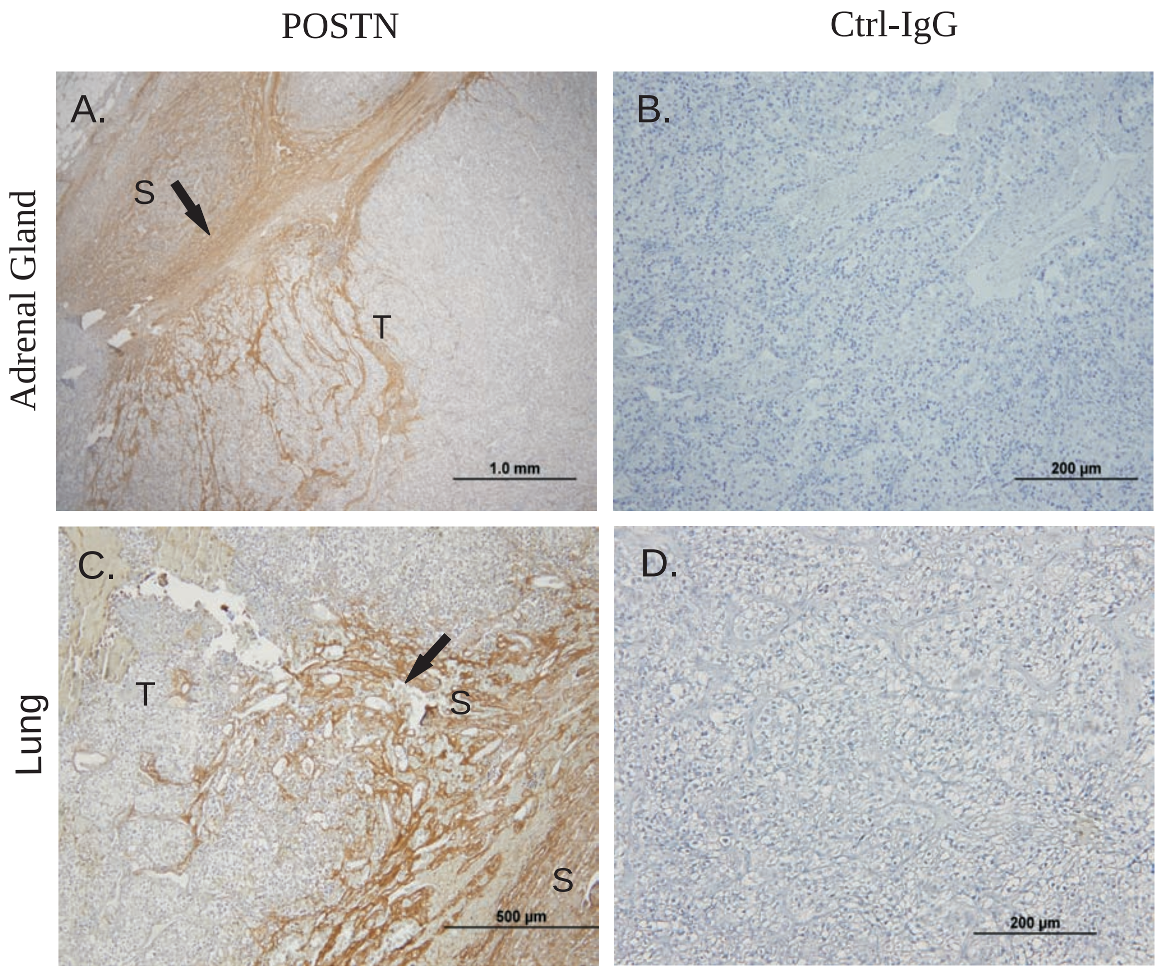

Figure 10: IHC analysis of invasive POSTN pattern from the stromal boundary into the tumour mass for metastatic ccRCC. **A, C)** POSTN expression in ccRCC metastasic to the adrenal gland and lung. **B, D)** Control (Ctrl) IgG for POSTN in adrenal gland and lung respectively. T**:** Tumour mass. S**:** Stromal region. Black arrows point to stroma.

4.3. Clear Cell RCC Induces Extracellular Accumulation of POSTN by Increasing Fibroblast POSTN Expression

4.3.1. Increase in Stromal POSTN Expression in ccRCC Xenograft Tumours

The kidney is not one of the main organs where POSTN is typically expressed. Therefore, the cellular origin of POSTN in ccRCC remains elusive (Horiuchi *et al*., 1999). To address the issue of POSTN origin in ccRCC, I took advantage of A498 ccRCC cells' low POSTN expression level, and investigated POSTN expression in A498 cell-derived xenograft tumours. IHC analysis revealed the presence of POSTN in the stroma within the tumour mass situated adjacent to non-tumour (N) tissue (Fig 11A). Furthermore, this tumour mass adjacent to non-tumour tissue appeared to be an invasive front of the tumour, protruding into the non tumour region (Fig 11A). This may indicate that POSTN aids in cell invasion. Moreover, POSTN protein was also expressed in the stroma of the boundary between tumour tissue and non-tumour tissue (Fig 11B). However, for the internal tumour (T) mass, POSTN was not detected in the stroma and tumour cells expressed very low levels of POSTN (Fig 11A). To confirm the tumour versus non-tumour region in our IHC analysis, we have detected blood vessels using von willebrand factor VIII antibody. Blood vessels were clearly present in the tumour mass and were enriched in the leading regions of tumour (Fig 11C, see xenograft tumour 1). This is consistent with the reported observation that a highly branched network of blood vessels is indicative of malignancy in tumour tissue when compared to non malignant tissue (Tlsty & Coussens, 2006). Collectively, we observed that A498 cells expressed low

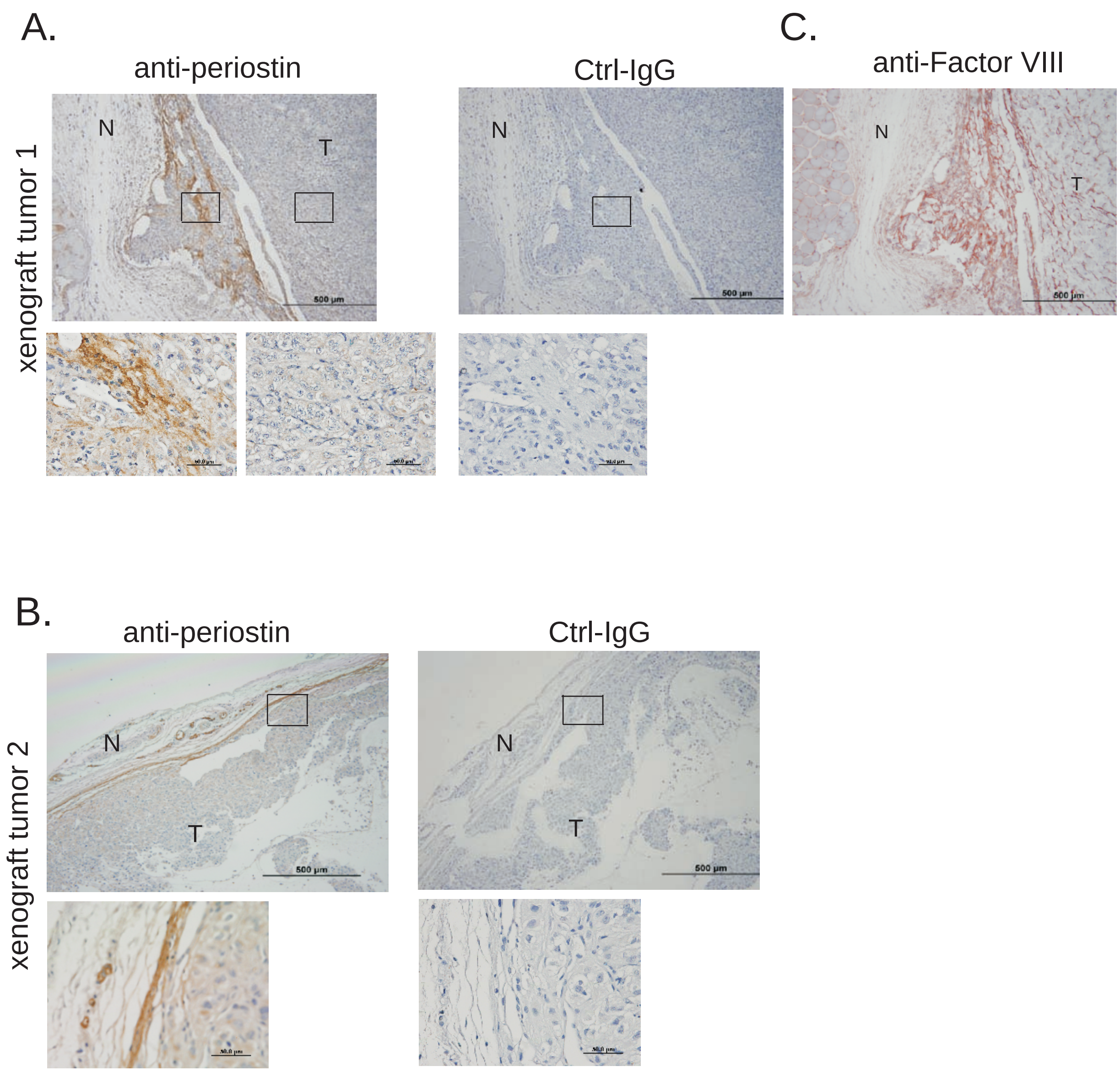

Figure 11. Stromal expression of periostin in two xenograft A498 ccRCC derived tumours. Please refer to Materials and Methods for details. Two xenograft tumours were analysed for periostin expression by IHC. N: non-tumour tissues; T: tumour mass. **A)** POSTN expression in the intra tumour stroma of xenograft tumour 1 with its Ctrl-IgG. **B)** POSTN in the stromal boundary between T and N of xenograft tumour 2 with matched Ctrl-IgG. **C)** Xenograft tumour 1 was also detected for blood vessels using an anti-factor VIII antibody. The boxed areas are images enlarged under higher magnification, and presented underneath the respective panels. Scale bars represent 500 µM and 50.0µm.

levels of POSTN in culture and in xenograft tumours, in addition, stromal POSTN was expressed at much higher levels in comparison to the tumour cells in the xenograft tumours. This suggests that the increase in POSTN may not have derived from tumour cells but originated from the stromal cells.

4.3.2. Periostin Expression Correlates with αSMA Expression

Our results thus far suggest that POSTN originates from the stromal cells. We wanted to consolidate the stromal origin and also obtain knowledge regarding the cell type in the stroma responsible for ccRCC-associated POSTN. Therefore, efforts were made to correlate stromal POSTN in ccRCC with cancer-associated fibroblast cells (myofibroblasts). This effort was based on our knowledge that fibroblasts comprise the majority of cells in the stroma, and that cancer cells induce resident fibroblasts into myofibroblasts (Abousshekra, 2011; Ronov-Jessen *et al*., 1995; Kojima *et al*., 2010). More importantly, myofibroblasts were detected in ccRCC stroma (Tanas *et al*., 2009; Bhuvarahamurthy *et al*., 2006). Therefore, to determine if POSTN is associated with myofibroblast cells, we performed dual IF on primary ccRCC tissue, ANK, and metastatic ccRCC tissue with the POSTN and αSMA antibodies. αSMA is the most common protein marker used to identify myofibroblast cells (Desmouliere *et al*., 2004). Our findings reveal that the ccRCC tumour tissue expresses more αSMA than ANK and that metastatic ccRCC displays a high level of αSMA. This is suggestive of more myofibroblast cells being present in ccRCC and metastatic ccRCC compared to ANK. Furthermore, αSMA was expressed in the same structural regions where POSTN fluorescence was detected (Fig 12A). This evidence indicates that the cells responsible for POSTN expression are the myofibroblast cells. This possibility is further supported by the observed co-existence of POSTN with fibronectin, a typical product of myofibroblasts (Fig 12B).

4.3.3. ccRCC Promotes Fibroblast Derived POSTN mRNA Expression

To provide direct evidence establishing the fibroblast-origin of stromal POSTN in ccRCC, we have co-cultured mouse NIH3T3 fibroblast cells with human A498 or 786-0 ccRCC cells and then analyzed POSTN mRNA by conducting semi-quantitative real time polymerase chain reaction (qRT-PCR). By taking advantage of the two different species, human ccRCC cells and mouse fibroblasts in this co-culture system, real time PCR primers specific for human and mouse POSTN targets were designed (Table 4). In comparison to single cultured A498 or 786-0 cells, human POSTN mRNA levels were not significantly altered when either A498 or 786-O cells were co-cultured with NIH3T3 cells (Fig 13A). In contrast, NIH3T3 cells co-cultured with either A498 or 786-0 cells significantly increased murine POSTN mRNA (Fig 13B). Collectively, these results demonstrate that NIH3T3 cells co-culture with A498 or 786-0 ccRCC cells resulted in upregulation of POSTN transcript levels in NIH3T3 fibroblasts (*$p < 0.05$, n=3).

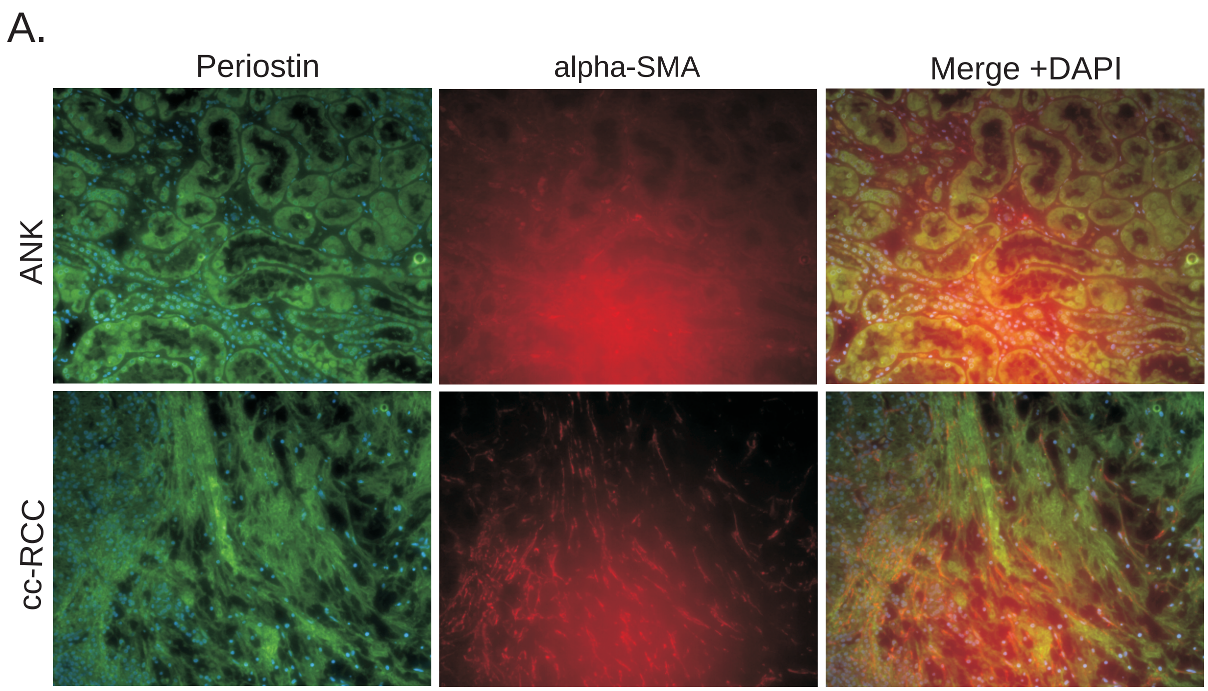
A.
Periostin
alpha-SMA
Merge +DAPI
ANK
cc-RCC

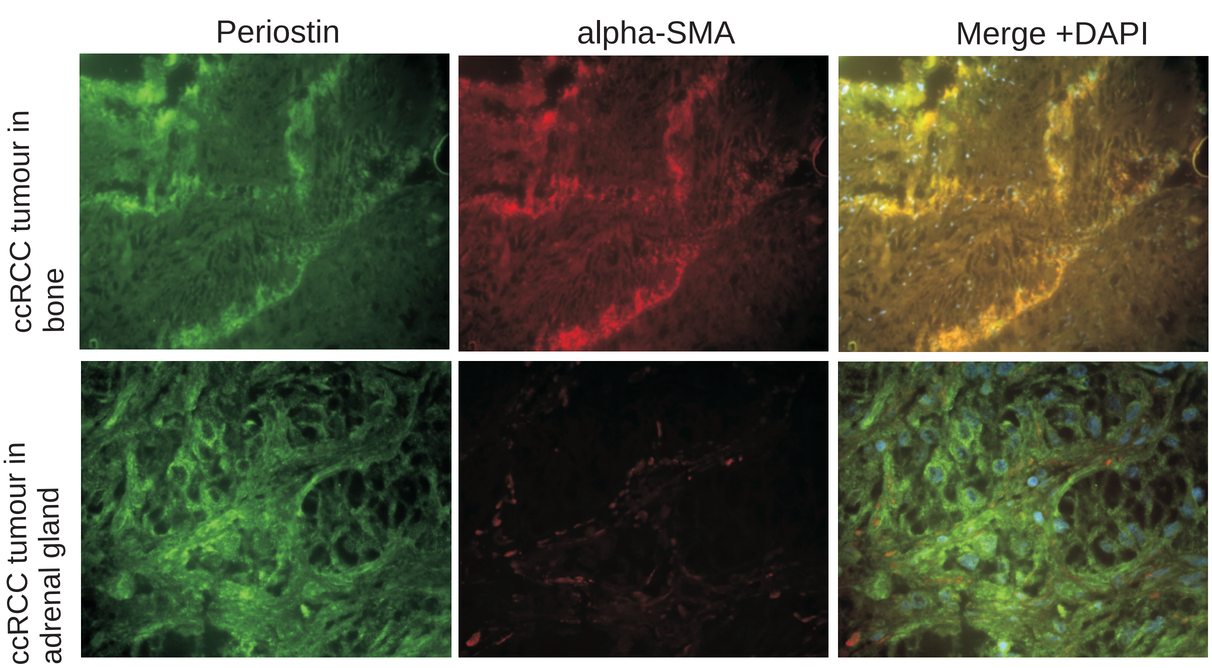
Periostin
alpha-SMA
Merge +DAPI
ccRCC tumour in bone
ccRCC tumour in adrenal gland

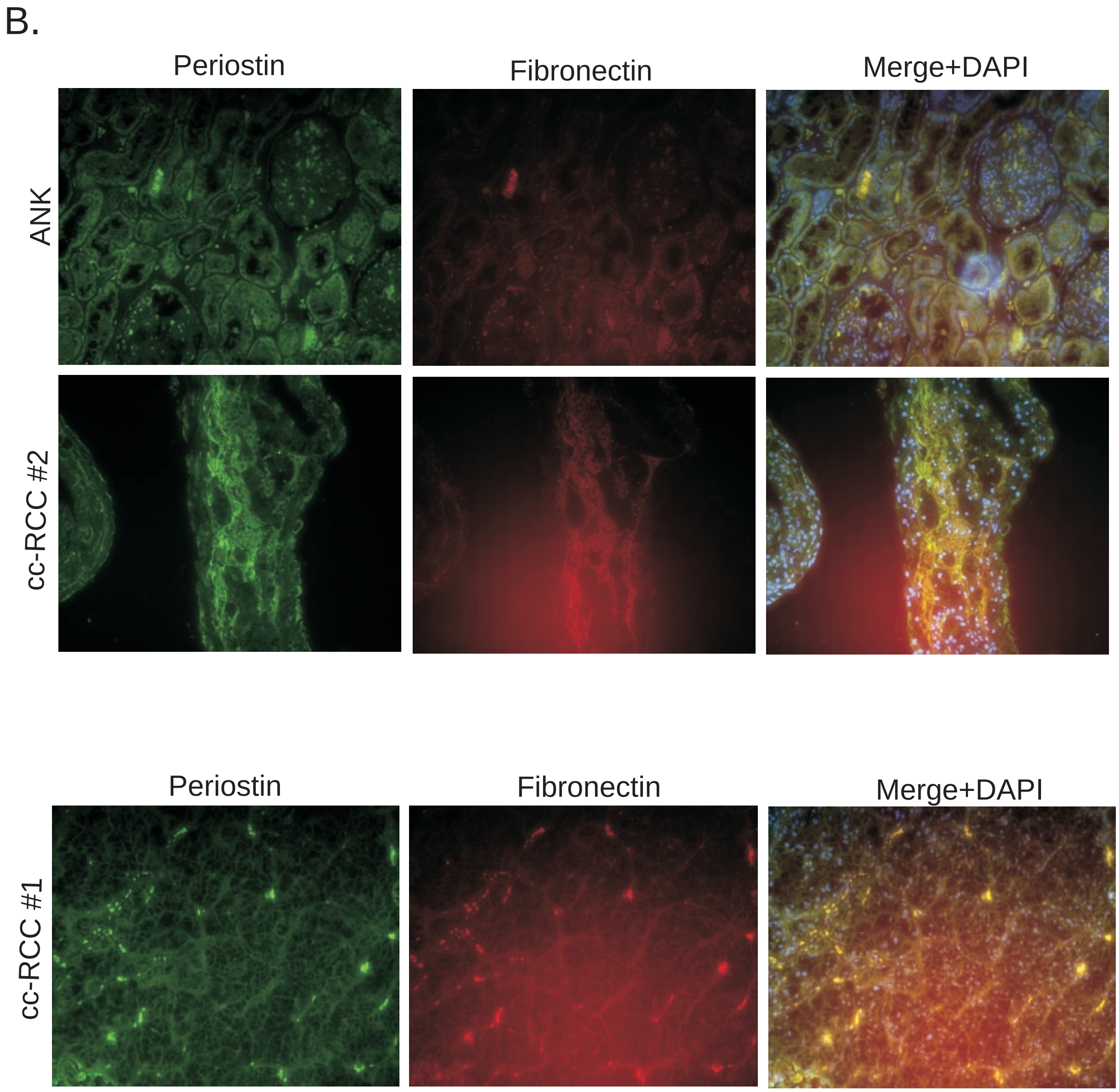

Figure 12: Dual IF conducted on ccRCC tumours and their respective ANK, including two cases of metastatic ccRCC to adrenal gland and bone. Dual IF antibodies used were POSTN and alpha-SMA or fibronectin. **A)** First column on the left displays POSTN FITC fluorescence in green. Second column displays alpha SMA cyb5 fluorescence in red. Third column displays both POSTN and alpha SMA dual IF with DAPI merge to display nuclei. **B)** Periostin and fibronectin dual IF for two patients with primary ccRCC. First column displays POSTN FITC fluorescence in green, second column displays fibronectin cyb5 fluorescence in red. Third column displays dual IF and DAPI merge.

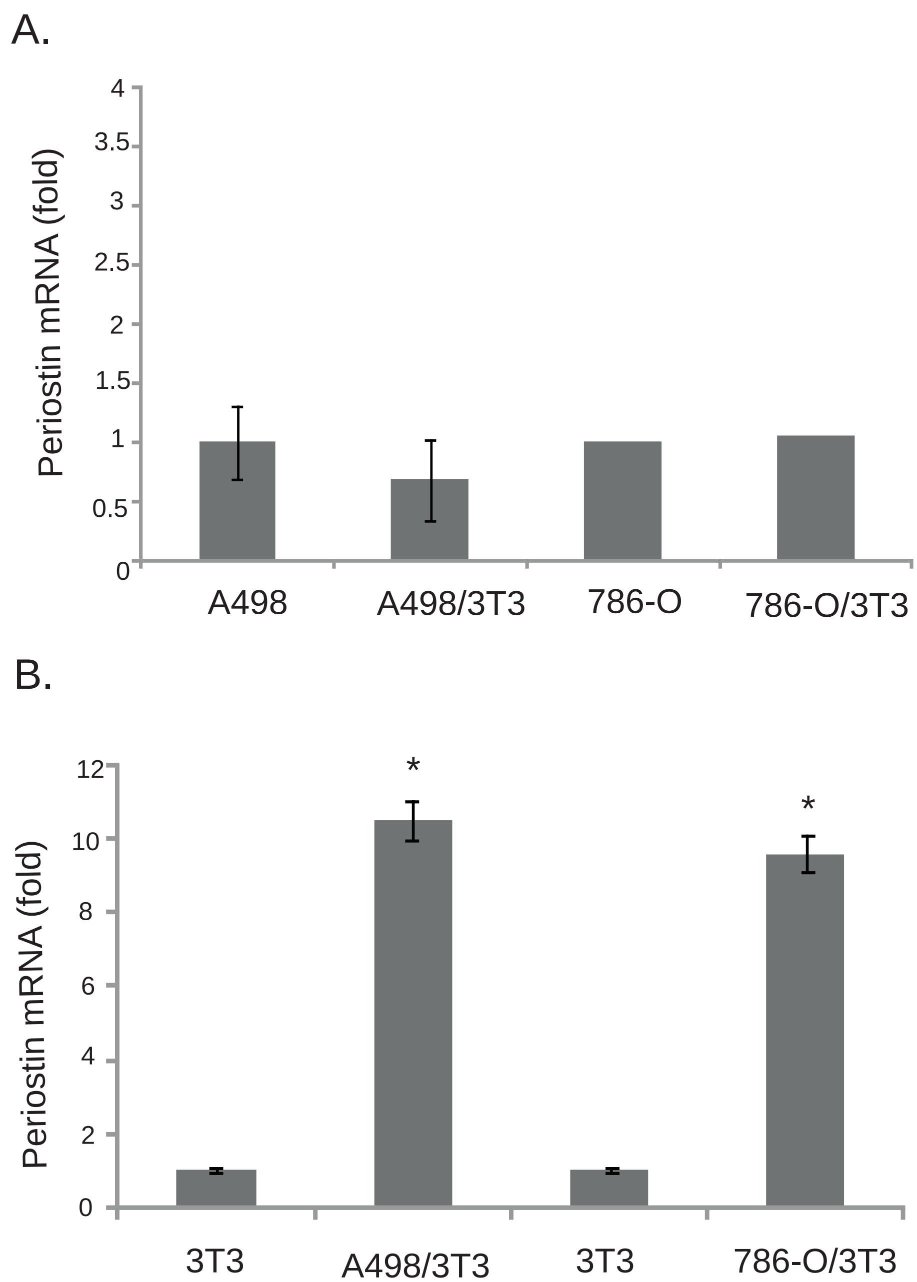

Figure 13. qRT-PCR analysis of a co culture experiment including murine NIH3T3 cells with ccRCC cells (A498/786-O). 3T3 cells and either A498 or 786-O cells were cultured in a 1:1 ratio till cells became 80-90% confluent. RNA was isolated and analyzed for human or mouse POSTN using species-specific primers. **A)** Using human POSTN primers, co culture did not result in an upregulation of POSTN transcript in comparison to single cultured ccRCC cells. **B)** Co culture of NIH3T3 with A498 or 786-O resulted in an amplification of murine POSTN. Experiments were repeated at least three times. Means ± SD (standard derivation) were graphed. * $p < 0.01$ in comparison to the specific NIH3T3 cells.

4.4. ccRCC Enhances Fibroblasts-Mediated Accumulation of Extracellular POSTN

POSTN is an extracellular adhesion protein (Shao *et al*, 2004; Tsunoda *et al*., 2009; Ruan *et al*., 2009) and we have observed a robust increase in stromal POSTN in both organ-confined and metastasized ccRCC. Furthermore, co-culture with human A498 or 786-0 ccRCC cells resulted in upregulation of the POSTN transcript in murine NIH3T3 cells. Our data collectively establishes that fibroblast cells increase their POSTN mRNA levels in response to ccRCC cells. Next we have examined whether upregulation of POSTN mRNA in fibroblasts contributes to the accumulation of extracellular POSTN.

4.4.1. POSTN is a Secreted Protein in NIH3T3 Cells

NIH3T3 cells express a low level of endogenous POSTN. To facilitate the examination of whether NIH3T3 cells are able to secrete POSTN, I have constructed NIH3T3 cells stably expressing ectopic FLAG-tagged POSTN. A POSTN cDNA was first inserted into a pcDNA3-CFLAG vector to add a FLAG tag to the C-terminus of POSTN. This FLAG tagged POSTN was then subcloned into a retroviral vector pLPCX. Empty vector (EV) and POSTN retrovirus were produced and used to stably infect NIH3T3 cells. Western blot analysis of whole cell lysates failed to detect ectopic FLAG tagged POSTN. This was likely attributable to the cellular POSTN not being accumulated to a certain level. This possibility was supported by the observation that immunoprecipitated ectopic POSTN from NIH3T3 POSTN whole cell lysates was recognized by the M2 anti-FLAG antibody (Fig 14A).

In an effort to directly examine whether POSTN is a secreted protein in NIH3T3 cells, I have collected 24 hour conditioned medium from NIH3T3 EV and POSTN cells. When 1/12.5 of 24 hour-conditioned medium was concentrated and analyzed on a western blot, abundant FLAG tagged POSTN was readily detected by both the M2 and anti-POSTN antibodies (Fig 14B). The amount of conditioned media run on western blot was proportional to that of the cell lysate examined. In this setting, actin was readily detected in the cell lysate but POSTN was not, and in the conditioned media POSTN was detected but actin was not (Fig 14B). This provides further evidence that the extracellular POSTN in the media was a product of secretion from NIH3T3 cells and had not resulted from cellular debris.

4.4.2. ccRCC Enhances Fibroblasts-Mediated Production of Extracellular POSTN

After demonstrating that POSTN is secreted from NIH3T3 cells, I wanted to determine whether co-culture of NIH3T3 with ccRCC cells leads to increases in the secretion of POSTN from the fibroblast cells. Western blot results demonstrate that NIH3T3 POSTN cells co-cultured with A498 or 786-O cells elevated the secretion of FLAG-tagged POSTN in comparison to ccRCC cells co-cultured with NIH3T3 EV or single cultured NIH3T3 POSTN cells (Fig 14C). These results also confirm the fibroblast origin of extracellular POSTN in the co-culture system.

To further elucidate if ccRCC cells can stimulate the secretion of endogenous POSTN from fibroblasts, I have co-cultured NIH3T3 cells with either A498 or 786-0

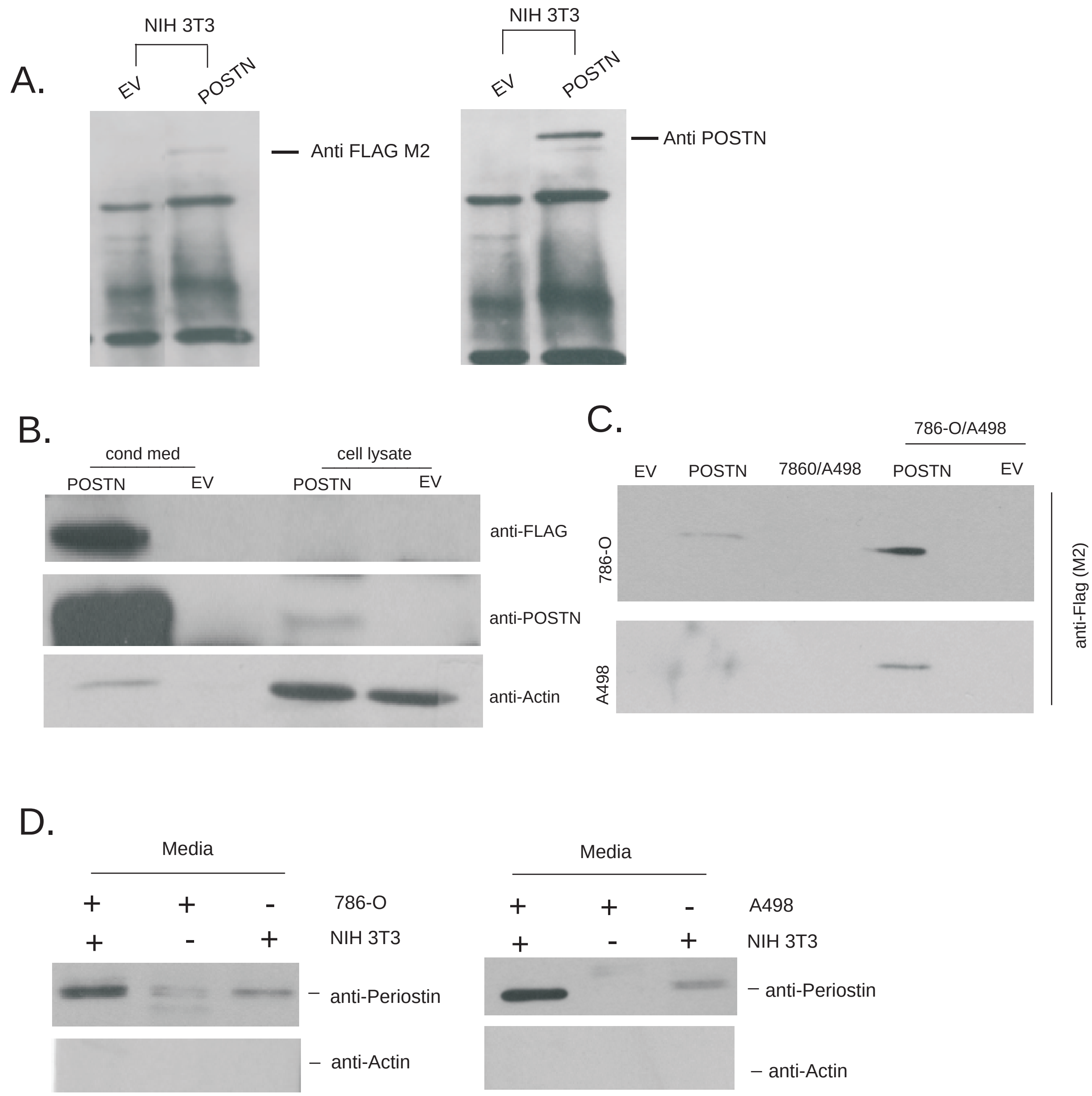

Figure 14: Periostin protein analysis using NIH3T3 Periostin (POSTN) and empty vector (EV) cells. **A)** Immunoprecipitation of retrovirus transfected NIH3T3 stable cells with FLAG- tagged POSTN and EV **B)** Cell lysate and conditioned medium were prepared. Approximately equal proportion of conditioned medium (1/12.5) and cell lysate were analyzed for POSTN and actin using the indicated antibodies. Cell lysates were from NIH 3T3 POSTN and EV cells. **C)** Clear cell RCC induces NIH3T3 fibroblast cells to produce extracellular POSTN. NIH3T3 EV and POSTN cells were either cultured alone or together with 786-0 (top panel) or A498 (bottom panel). Conditioned medium were harvested (see Materials and Methods for details) and analyzed for ectopic POSTN using the M2 anti-FLAG antibody. **D)** NIH 3T3 cells were either cultured alone or together with A498 or 786-0 cells to analyze periostin at the mRNA and protein level. NIH3T3 and A498 cells were cultured in the indicated combinations, followed by western blot analysis of conditioned media using anti-periostin antibody and anti-actin antibody.

ccRCC cells. Western blot results of the conditioned media revealed that A498, 786-0 and NIH3T3 cells by themselves secreted negligible amounts of POSTN. However, co-culture of NIH3T3 cells with either A498 or 786-O cells significantly enhanced the secretion of POSTN (Fig 14D). These observations are thus consistent with the qRT-PCR results where upregulation of the POSTN mRNA in NIH3T3 cells was detected in response to the presence of A498 or 786-O ccRCC cells.

4.5. Extracellular Periostin Enhances A498 ccRCC Cell Attachment

POSTN is an extracellular adhesion molecule. The observation that ccRCC cells enhanced the extracellular accumulation of fibroblast-derived POSTN suggests that stromal POSTN may promote ccRCC attachment. To examine this possibility, recombinant POSTN or glutathione S-transferase (GST) recombinant protein was used to coat petri dishes. Petri dishes unlike tissue culture plates are not chemically treated, and hence do not support cell adhesion. A498 cells were allowed to attach to the POSTN and GST coated petri dishes for 45 minutes. Non-adherent cells were then gently removed by changing the media. To enhance cell attachment, the adherent cells were incubated in a 37^{o}C tissue culture incubator for 5 hours. The cells were then washed, fixed in fixing solution and stained with crystal violet. In comparison to the control, GST-coated petri dishes, a significantly higher number of cells attached to POSTN-coated petri dishes. On average, (162.2 ± 19.275, p=2.82E-10) cells adhered to the GST coated plate, while (341.4 ±15.003, p=2.82E-10) cells adhered to the POSTN coated plate (* $p < 0.01$, n=3) (Fig 15A).

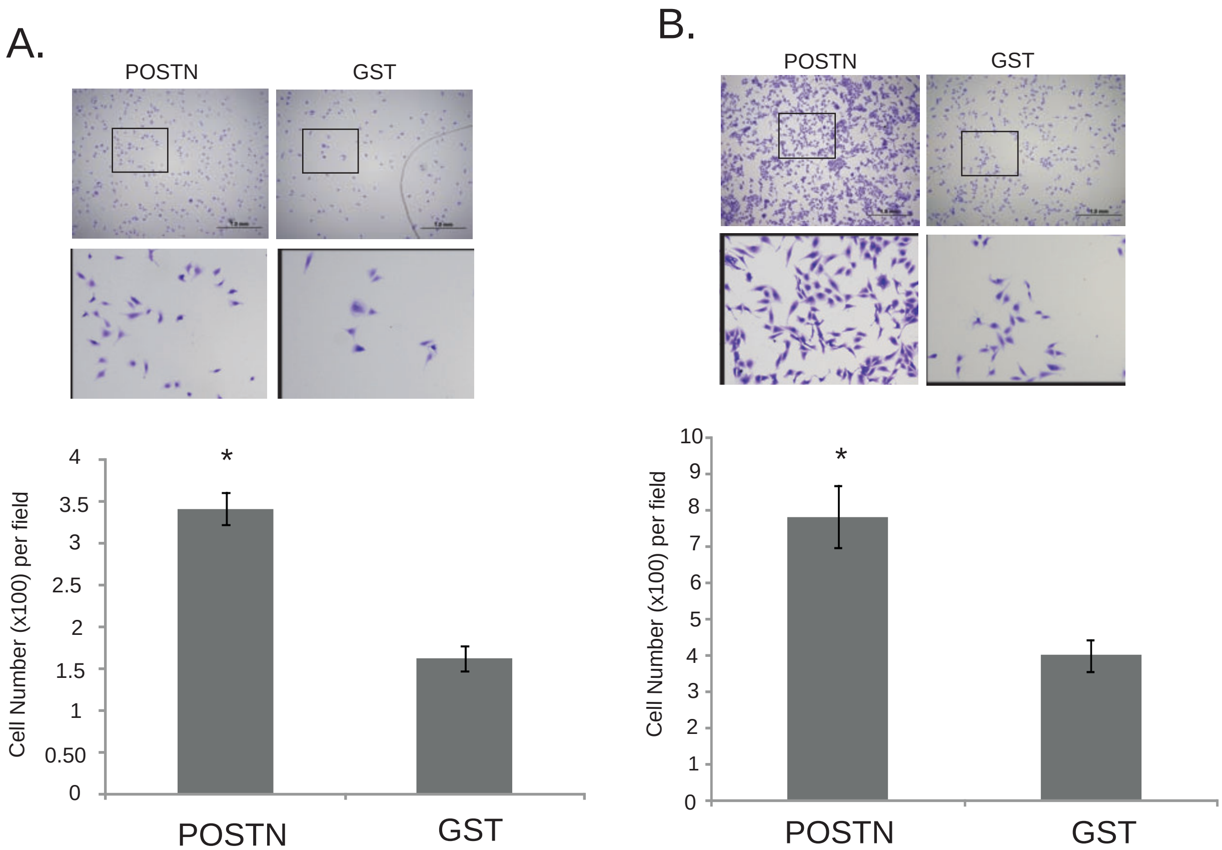

Figure 15. Extracellular POSTN enhances A498 ccRCC cell attachment. Petri dishes were either coated with GST or recombinant POSTN (see Materials and Methods for details). **A)** Cells (4×10^4) were allowed to attach for 45 minutes, followed by removing non-adherent cells and addition of medium containing 2% FBS for 5 hours to increase their attachment. Cells were then stained with 0.5% crystal violet. Six random images were taken for a given plate. Typical images are shown (top). The boxed areas were enlarged 3.2 fold and placed underneath the respective panel. Experiments were repeated three times. Average number of cells per field [Means ± SD (standard derivation)] was graphed. * $p < 0.01$ in comparison to Ctrl dishes. **B)** Cells were attached as described in panel **(A)** and cultured for 2 days. Cells were then stained with 0.5% crystal violet. Six random images were then taken using the same magnification as that used in panel **(A)**. Typical images are shown (top). The marked regions were enlarged 3.2 fold and placed underneath. Average number of cells per field (Means ± SD) was graphed. * $p < 0.01$ in comparison to Ctrl dishes.

We subsequently examined whether the A498 cell attachment on POSTN coated petri dishes support functional adhesion, which is defined as adhesion supporting cell proliferation. For this purpose, we cultured the 45 minutes adherent cells for 2 days and then fixed and stained the cells in order to record cell number. The average number of cells in six randomly selected fields were (402 ± 86.065, p=6.222E-9) and (784 ± 44.337, p=6.222E-9) for GST and POSTN-coated petri dishes, respectively (Fig 15B). Taken together, the above observations demonstrate that extracellular POSTN supports functional attachment in terms of cell proliferation (* $p < 0.01$, n=3).

4.6. High Levels of Ectopic Periostin Enhances Fibroblast Cell Attachment, Growth and Migration

To further characterize POSTN function, we have assessed the impact of elevated POSTN on fibroblast cell attachment and proliferation. To mimic the ccRCC cell-induced upregulation of POSTN in NIH3T3 cells, we used the NIH3T3 POSTN cell line. Since PONTN is secreted from NIH3T3 cells, we performed the above cell-attachment experiments for NIH3T3 EV and NIH3T3 POSTN cells using un-coated petri dishes. Once again, the cells were allowed to adhere for 45 minutes followed by a media change and then 5 hours of incubation in a 37^{o}C incubator. For NIH3T3 EV cells, an average of (21.28±11.801, p= 0.00258) cells had adhered, whereas an average of (307.17±11.8333, p=0.00258) NIH3T3 POSTN cells had adhered to the petri dish (Fig 16A). As FLAG tagged POSTN in NIH3T3 cells were readily secreted out, the above results indicate that the secreted form of POSTN enhances NIH3T3 cell adhesion (*$p<0.01$, n=3).

A variety of cancers, including ccRCC, have been shown to activate resident fibroblasts into myofibroblasts. Active fibroblasts or myofibroblasts are associated with increased proliferation potential in comparison to resident fibroblasts (Tanas *et al*., 2009). In addition, it has been reported that POSTN enhanced pancreatic cancer proliferation (Ben *et al*., 2011). Consistent with this report, we were able to show that when seeded at low densities of 100, 500 and 1000 cells, NIH3T3 POSTN fibroblast cells formed substantially more colonies than NIH3T3 EV cells (Fig 16B, C). The average number of colonies for 1000 cells were (POSTN: 121±13.928, EV: 68.33±3.399, p=0.00654), for 500 cells (POSTN: 71.66 ±6.944, EV: 36.33±3.682, p=0.00317) and for 100 cells (POSTN: 38.33±4.027, EV: p=12.33± 6.944, p=0.0101). These results suggest that NIH3T3 POSTN cells have a higher proliferation rate than NIH3T3 EV cells. Collectively, these observations are in line with the concept that ccRCC cells activate resident fibroblasts, in which elevated POSTN play s a role (*p< 0.05, n=3).

To consolidate this notion, we have examined the migration capacity of NIH3T3 EV and NIH3T3 POSTN cells. The wound healing assay showed that NIH3T3 POSTN cells closed the gap/wound faster than NIH3T3 EV cells (Fig 17). As myofibroblasts are well-known to be more invasive compared to resident fibroblasts (Tlsty & Coussens, 2006), the above observations support the concept that POSTN plays a role in the activities of the ccRCC induced myofibroblasts.

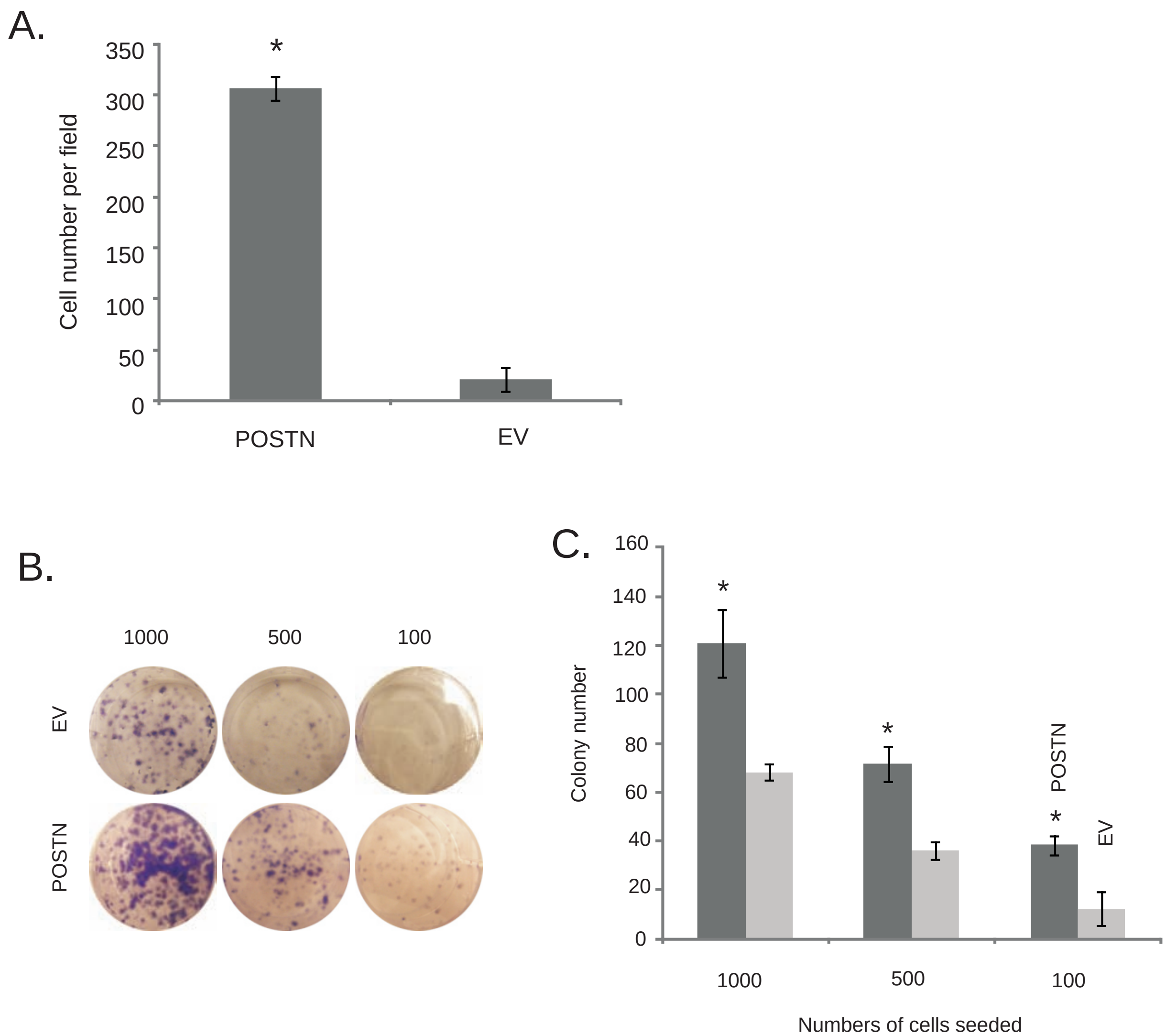

Figure 16. High levels of POSTN increase NIH3T3 cell growth. **A)** NIH3T3 EV and POSTN cells were attached on (uncoated) petri dishes as described in Fig 15A legend. Cells from 6 random fields were counted. Experiments were repeated three times. Average number of cells per field (Means ± SD) was graphed. * $p < 0.01$ in comparison to EV cells. **B)** NIH3T3 EV and POSTN cells were seeded in 6 well tissue culture plates at the indicated number per well and cultured for a week till colonies were clearly visible. Cell colonies were then stained with 0.5% crystal violet. Experiments were repeated at least three times. Typical images from a repeat were shown **(B)** and quantified (Means ± SD) (**C**). * $p < 0.05$ in comparison to the respective EV cells.

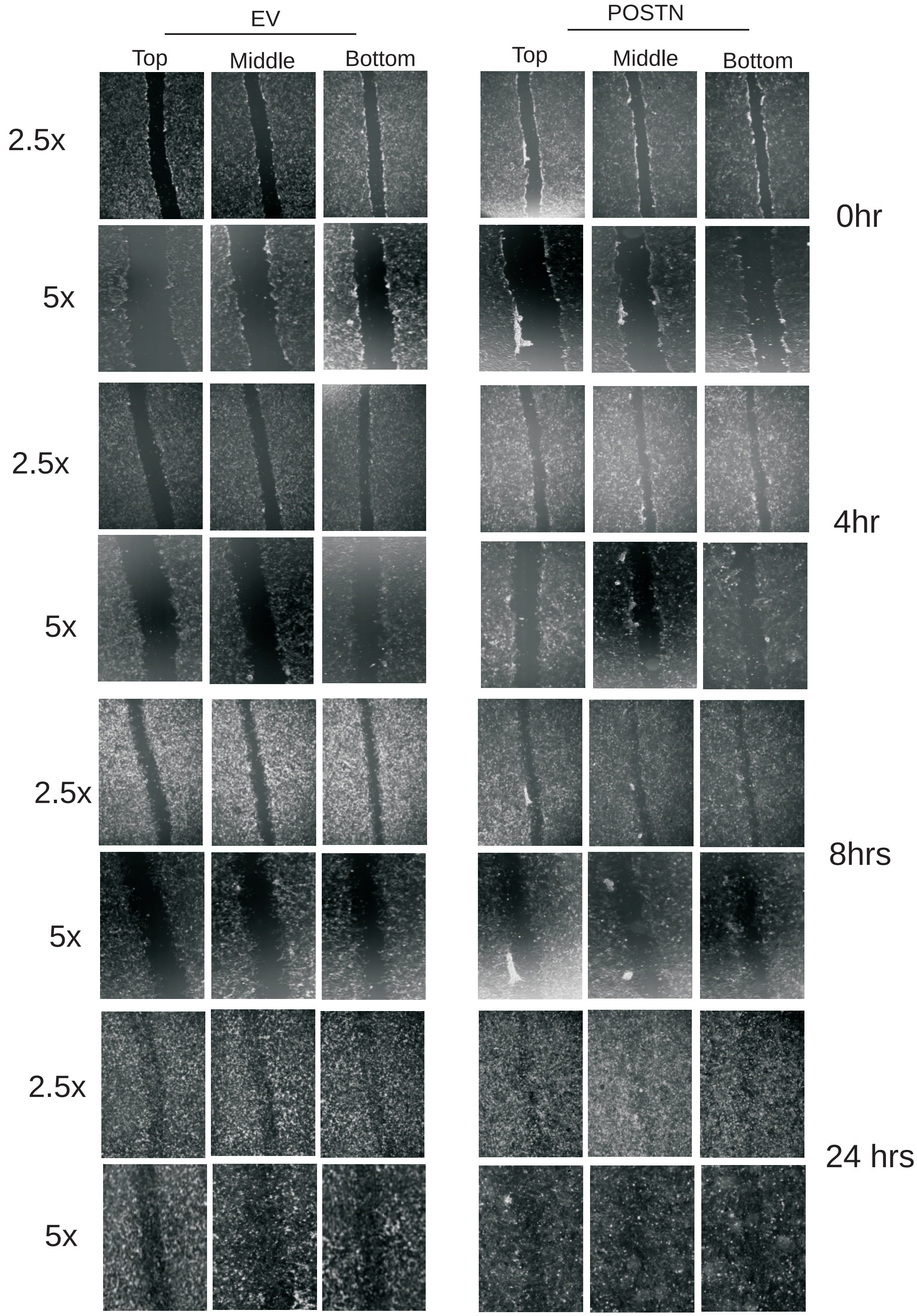

Figure 17. Wound healing assay using the NIH3T3 EV and POSTN over expression cell lines. Over time NIH3T3 POSTN cells closed the wound at a faster rate than EV cells. Images were taken at time points 0hrs, 4hrs, 8hrs and 24 hrs and were captured from the top, middle and bottom regions of the vertical scratch. These images were obtained under 2.5x low magnification to illustrate the over all scratch diameter changes over time. Images were also taken under 5x magnification to display the movement of cells into the wound as the wound is healed.

4.7. Periostin Overexpression Activates the PI3K/AKT Pathway in NIH3T3 cells

POSTN was reported to activate AKT in cancers of the colon and pancreas (Bao *et al*., 2004; Baril *et al*., 2007). Our observations that POSTN enhances NIH3T3 cell proliferation and migration suggest that POSTN may mediate these processes via activation of AKT. Consistent with this possibility, western blot analysis revealed an elevation in AKT phosphorylation in NIH3T3 POSTN cells in comparison to NIH3T3 EV cells (Fig 18). Additionally, GSK-3β Ser9 phosphorylation, a well regarded AKT substrate, was also elevated in NIH3T3 POSTN cells in comparison to the NIH3T3 EV cells (Fig 18). Furthermore, increase in p70S6K phosphorylation was observed in NIH3T3 POSTN cells. It is well established that AKT activates mTOR, leading to mTOR-mediated phosphorylation of p70S6K, a process which initiates protein translation (Vivanco *et al*., 2006). Taken together, the above observations reveal that elevated POSTN activates AKT in the NIH3T3 cells and that AKT activation in turn leads to the activation of downstream targets reported to be involved in cancer progression.

4.8. Periostin as a Potential Angiogenesis Inducer in ccRCC

POSTN has been reported to play a critical role in promoting angiogenesis in several different human cancers (Ruan *et al*., 2009). To examine whether POSTN correlates with blood vessel formation in ccRCC, we performed IHC analysis on serially sectioned ccRCC slides for von willebrande factor VIII protein and POSTN protein.

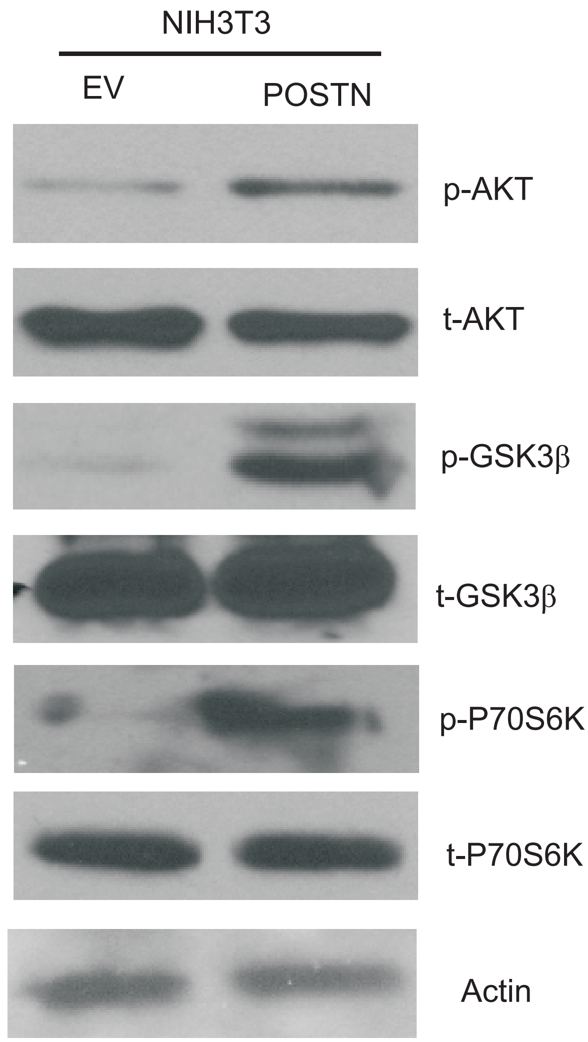

Figure 18. Western blot analysis of PI3K/AKT pathway. NIH3T3 POSTN and NIH3T3 EV whole cell lysates were used for western blot analysis. POSTN over expressing NIH3T3 cells have enhanced AKT phosphorylation (p-AKT) when compared to EV cells. NIH3T3 POSTN cell lysates also displayed higher level of p-GSK3β and p-P70S6K levels when compared to EV cells. Respective total AKT, GSK3β and P70S6K levels are represented under the phosphorylated protein results. Actin was the loading control.

While some co-localization could be detected, a convincing co-localization could not be demonstrated (Fig 19A). This might be attributable to difficulties in finding corresponding areas in serially sectioned slides. To overcome these complications, a dual immunofluorescence protocol was followed. The results illustrate some overlap between the two antibodies (Fig19B), indicating that POSTN is present in the vessels where factor VIII is also expressed. However, further experimentation is necessary to examine the correlation between factor VIII and POSTN.

4.9. Serum Levels of Periostin do not Associate with ccRCC Tumorigenesis

Consistent with our current understanding that extracellular POSTN contributes to the protein's physiological function (Ruan *et al*., 2009; Morra *et al*., 2011), an increase in serum levels of POSTN was detected in patients with bone-metastasized breast cancer (Contie *et al*., 2011). Additionally, higher preoperative serum POSTN levels were reported in patients with metastatic and advanced colorectal cancer (Ben *et al*., 2009).

To assess a potential correlation between serum levels of POSTN and ccRCC, we have conducted ELISA experiments using serum obtained from 24 ccRCC patients (Table 1) and two volunteers. Repeated ELISA analysis did not detect increase in serum POSTN in any ccRCC patients in comparison to two normal control individuals (Fig 20). It has been reported that POSTN is secreted in detectable amounts into the serum in patients with metastatic breast (Contie *et al*., 2011) and advanced colorectal cancer (Ben *et al*., 2009). Since the sera in our patient cohort were not derived from patients with metastatic ccRCC, it remains a possibility that the serum level of POSTN may become detectable in advanced or metastatic ccRCC patients. Furthermore, our ELISA experiment was performed following the same sandwich ELISA conditions and using the same POSTN detection antibody (Abcam 14041) as utilized by Ben and his lab (Ben *et al*., 2009). Hence our experimental conditions are comparable to those reported, suggesting that the lack of POSTN detected in the ccRCC patient serum is not attributable to our ELISA protocol.

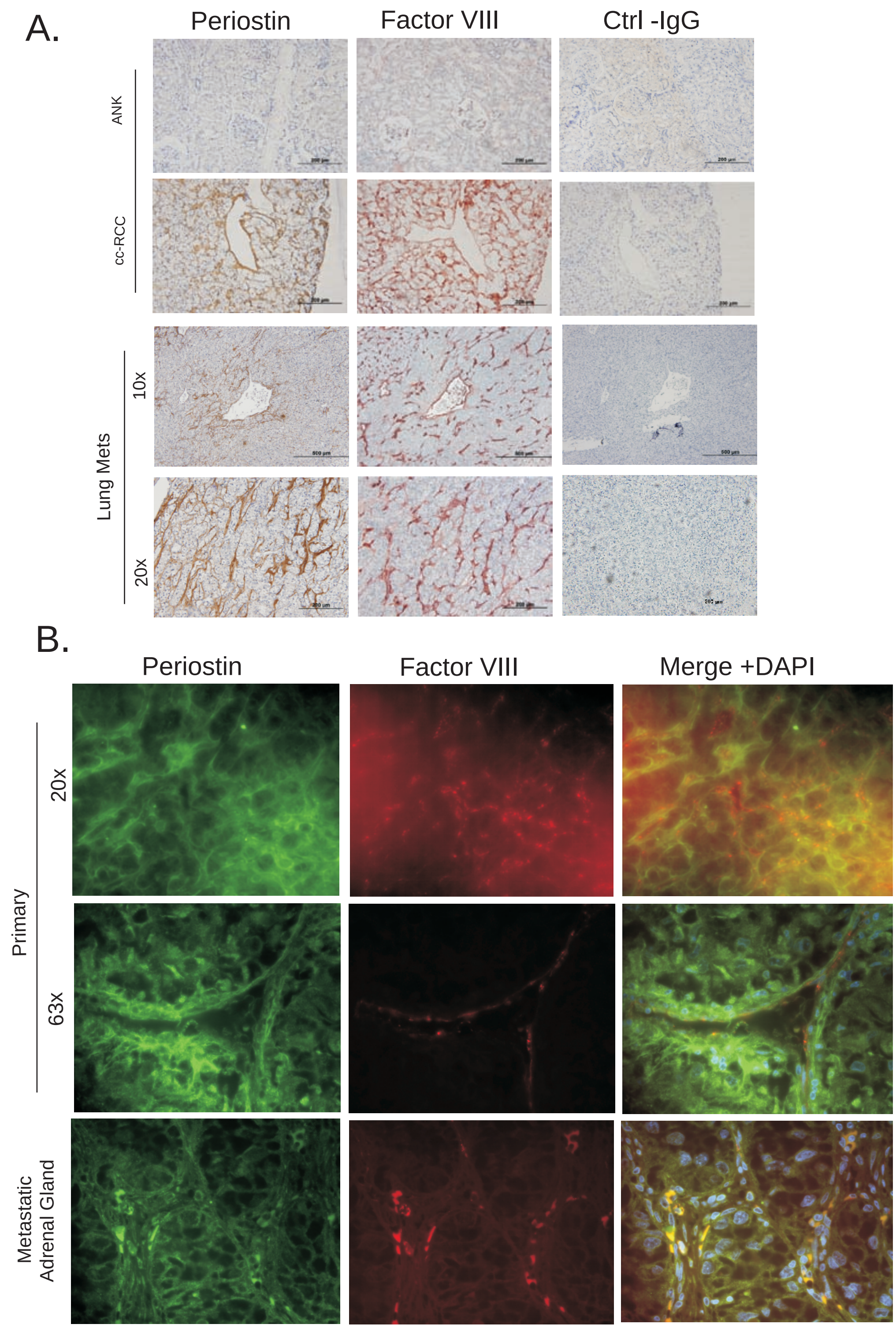

Figure 19: Periostin and factor VIII detection using IHC and IF. **A)** IHC analysis of periostin and factor VIII proteins on serially sectioned ccRCC slides, each set uses two consecutive sildes. Top two panels demonstrate ccRCC and its respective ANK tissue. Lower two panels represent metastatic ccRCC to lung. 10x and 20x magnification. IgG was used as a control. **B)** Dual IF using periostin and Factor VIII antibodies. First column displays green FITC fluorescence for POSTN antibody. Second column displays red cyb5 fluorescence using factor VIII antibody. Third column represents merge of the dual fluorescences and DAPI used to probe nuclei.

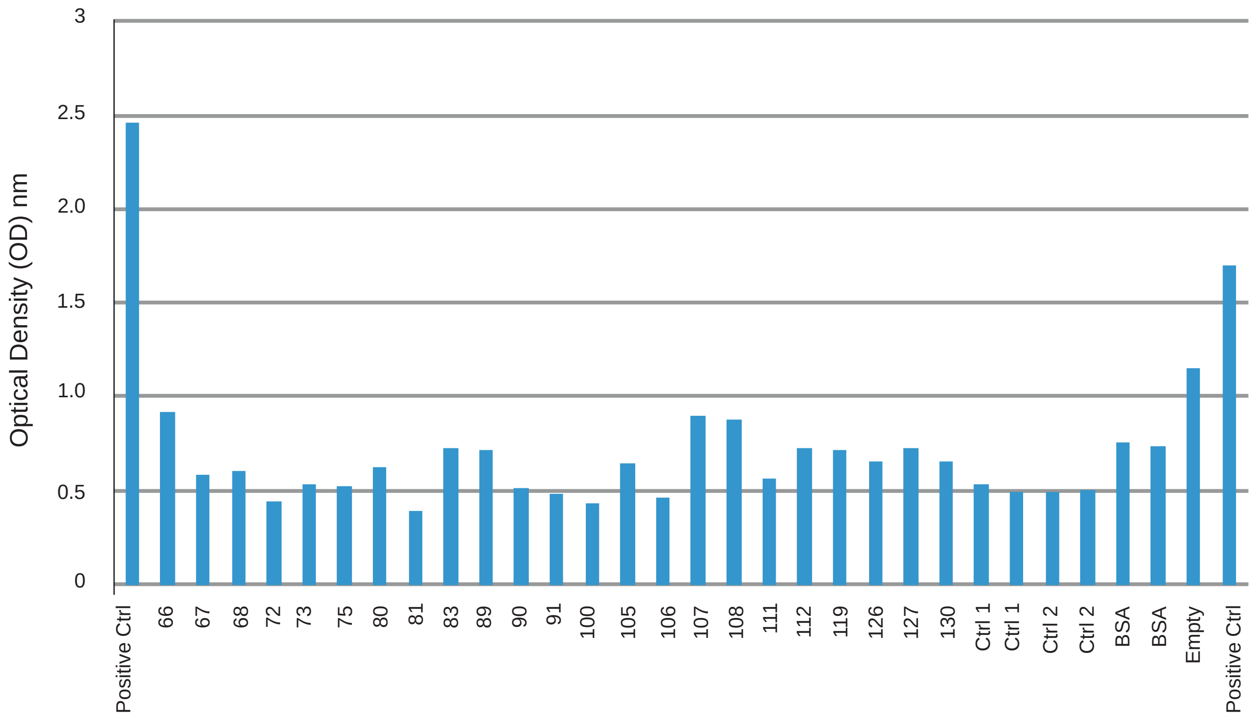

Figure 20: ELISA experiment of cc-RCC patient's serum do not associate with an increase in serum periostin. Sera were obtained from indicated patients (Table1) and two volunteers (Cntrl1/2). Absorbance was detected at 450nm. Y axis displays absorbance levels. Recombinant periostin was used as a positive control. Experiments were repeated atleast 3 times.

V. DISCUSSION

Clear cell RCC represents 75-80% of the cases of RCC and it is also the most aggressive form of RCC (Linehan, Walther, & Zbar., 2003; Nelson *et al*., 2007). Clear cell RCC is associated with a high risk of metastasis and metastasized ccRCC remains incurable. While early detection is vital to prevent ccRCC from progressing into metastasis, early diagnosis remains a challenge as ccRCC is normally asymptomatic (Nelson *et al*., 2007; Brugarolas *et al*., 2007). The current situation is largely attributable to our lack of understanding of ccRCC pathogenesis. This calls for the identification of novel oncogenic factors to provide insight into ccRCC development.

Despite being a critical contributor of tumorigenesis, the influence of the tumour microenvironment on tumour formation and pathogenesis is a less well characterized oncogenic process. Tumorigenesis of solid tumours, including ccRCC, is a co-evolving process between cancer cells ("seeds") and the stroma ("soil"). While extensive research efforts have been devoted to researching the "seeds", investigation of the "soil" falls far behind. This situation is also applicable to ccRCC. One of these possible stromal contributors to ccRCC could be POSTN. Upregulation of POSTN was reported in various cancers, including lung (Soltermann *et al*., 2008), esophagus (Michaylira *et al*., 2010), colon (Bao *et al*., 2004), liver (Utispan *et al*., 2010), pancreas (Baril *et al*., 2007), ovary (Gillian *et al*., 2002; Zhu *et al*., 2010), breast (Shao *et al*., 2004; Puglisi *et al*., 2008), and prostate (Tsunoda *et al*., 2009; Tischler *et al*., 2010). More importantly, POSTN is an extracellular protein, which suggests that it could contribute to ccRCC via modulation of ccRCC microenvironment or the soil.

Accumulating evidence states that POSTN functions in the development and homeostasis of bone, teeth, and heart (Ruan *et al*., 2009; Kudo, 2011). In addition to these physiological functions, recent development clearly reveals POSTN's involvement in tumour progression (Ruan *et al*., 2009; Morra *et al*., 2011). Although POSTN was reported to inhibit bladder cancer (Kim *et al*., 2005; Isono *et al*., 2009), POSTN is upregulated and correlates with cancer progression in a variety of human cancers (lung, liver, colon, pancreas, prostate, breast, ovary, and kidney). However, the mechanisms leading to POSTN upregulation in many human cancers remains unclear. In ccRCC, we have shown that stromal POSTN is produced by fibroblasts in response to ccRCC tumour cells.

5.1. The Extracellular Presence of Periostin and its Function

We were initially unable to detect our FLAG-tagged POSTN in NIH3T3 cells through western blot analysis of whole cell lysates. POSTN has been reported to function as a secreted protein in osteoblasts and osteoblast like cells (Takeshita *et al*., 1993). It was thus possible that in the NIH3T3 POSTN cells, POSTN was being secreted. In our subsequent examination of conditioned media, POSTN was readily detected. This would suggest that the reason for the presence of low levels of cellular POSTN in NIH3T3 POSTN cells might be attributable to the active secretion of POSTN. However, this does not exclude the possibility that cellular POSTN may also have been subjected to active degradation. Further experiments may need to examine the half-life of cellular POSTN. This can be accomplished by conducting a pulse chase experiment. In a pulse chase amino acids are metabolically labelled with isotopes. By monitoring the kinetics of reduction of the labelled POSTN in the chase phase, the half-life of POSTN can be determined.

As an extracellular matrix protein, POSTN promotes cancer cell motility and invasion (Ruan *et al*., 2009; Morra *et al*., 2011). Additionally, extracellular POSTN functions in maintaining niches for homing breast cancer stem cells during metastasis (Malanchi *et al*., 2012; Wang *et al*., 2012). Collectively, evidence from literature demonstrates an oncogenic role for extracellular POSTN. Consistent with this understanding, in contrast to weak POSTN expression inside the tubular epithelial cells in the adjacent non-tumour kidney tissues, ccRCC is predominantly associated with stromal POSTN. While the stromal POSTN plays a critical role in maintaining niches for breast cancer stem cells (Malanchi *et al*., 2012; Wang *et al*., 2012), stromal POSTN may have an additional role in ccRCC pathogenesis. This interpretation is based on our results demonstrating the presence of stromal POSTN in local and metastasized ccRCC (Figs 6A, 8, 9). In addition, the report by Malanchi *et al*. shows that POSTN deficiency reduced breast cancer metastasis but did not affect the formation of organ-confined breast tumours (Malanchi *et al*., 2012). Our results demonstrate that there is an abundance of stromal POSTN expression in both local and metastatic ccRCC, suggestive of POSTN playing a role in both primary and metastatic ccRCC progression (Figs 6A, 8, 9). The concept that stromal POSTN promotes ccRCC is consistent with our observations that POSTN was not detected in the stroma of pRCC, but remained inside of the pRCC tumour cells (Fig 6B). In addition, POSTN was not upregulated in pRCC western blot analysis in comparison to

ANK. On the other hand, intracellular POSTN may also contribute to pathogenesis of pRCC, perhaps through different mechanisms. This possibility is consistent with the recent development showing that intracellular POSTN plays a role in fibrillogenesis by enhancing collagen cross link formation necessary for fibrillogenesis (Kudo, 2011).

5.2. The Secretion of POSTN by Stromal Fibroblasts

We have demonstrated through *in vitro* co-culture experiments that ccRCC cells induce fibroblast cells to produce and secrete POSTN. These results support the possibility that the stromal POSTN in ccRCC tumours was most likely derived from the stromal fibroblast cells. This conclusion was based on the observations that **1)** low levels of endogenous POSTN was detected in a panel of ccRCC cells; **2)** In A498 cell-derived xenograft tumour, internal ccRCC cells do not express detectable POSTN. However, POSTN was detected in tumour mass adjacent to the non-tumour regions and in the boundary between xenograft tumour mass and non-tumour stroma (Fig 11). This offers *in vivo* evidence that ccRCC cancer cells may not express POSTN at high levels but instead induce fibroblasts to produce POSTN. This is of critical importance because it shows that the stroma of ccRCC tumour is altered by ccRCC cells. This is consistent with reports stating that cancer cells can produce stroma-modulating factors (Mueller & Fusenig, 2004) that lead to the stromal production of secreted proteins. These stromal proteins in turn may promote ccRCC progression. We have shown that POSTN is one such protein. **3)** Co-culture of NIH3T3 cells with either A498 or 786-0 ccRCC cells significantly increased POSTN transcript levels by NIH3T3 fibroblast cells. Co-culture also resulted in the extracellular accumulation of NIH3T3 cell-derived POSTN.

The ccRCC enhanced stromal presence of POSTN is at least in part due to increasing the abundance of POSTN mRNA. Whether this increase was due to up regulating POSTN transcription or stabilizing POSTN mRNA needs further investigations. Additionally, we cannot exclude the possibility that ccRCC also increases the secretion process of POSTN by fibroblast cells. Our research is consistent with a recent report that breast cancer induced stromal POSTN (Malanchi *et al*., 2012).

The fibroblast cells of the stroma are able to transition into myofibroblasts. This transition process can be induced by tumour cells (De Wever *et al*., 2000; Sappino *et al*., 1990). Myofibroblasts have a higher proliferative index, recruit inflammatory cells, and activate angiogenic programs (Tlsty & Coussens, 2006). Our observed co-localization between POSTN and αSMA in both organ-confined and metastasized ccRCC (Fig 14) indicates that the cellular origin of POSTN is myofibroblast.

5.3. Periostin Promotes Cell Adhesion and Growth

By using petri dishes, we demonstrated that extracellular POSTN enhances the attachment and growth of ccRCC and NIH3T3 POSTN fibroblast cells. Functional cell adhesion is an important step in both primary tumour formation and in metastases during tumour cell homing to secondary organs. In comparison to GST-coated petri dishes, immobilized POSTN enhanced A498 cell attachment by 2.1 fold (162.2 cells for GST-plates vs 341.1 for POSTN-plates). On the other hand, more than 14 fold of NIH3T3

POSTN cells attached to petri dishes in comparison to NIH3T3 EV cells (307.17 PONSTN cells vs 21.28 EV cells). While multiple factors may have contributed to the more efficient attachment of NIH3T3 POSTN cells in reference to the A498 cells on POSTN-coated plate, one intriguing possibility is that POSTN secreted by NIH3T3 cells is perhaps more efficient in supporting cell adhesion than purified recombinant POSTN. It would be interesting to coat petri dishes with conditioned medium derived from EV or POSTN NIH3T3 cells and then examine the attachment properties of A498 cells.

In comparison to NIH3T3 EV cells, NIH3T3 POSTN cells are more proliferative and motile and display elevated AKT activation, suggesting a role of AKT activation in the POSTN-induced proliferative and motile functions. In addition, NIH3T3 POSTN cells display elevated GSK3β and P70S6K phosphorylation. GSK3β phosphorylation is known to induce epithelial to mesenchymal transition (EMT) and P70S6k phosphorylation leads to protein translation and hence cell proliferation (Qiao *et al*., 2008). These observations are in line with the reports that matrix POSTN promotes cancer cell motility, EMT, metastases and angiogenesis (Morra & Mock, 2011). High proliferation rate of activated fibroblasts is important in cancer because this leads to the formation of desmoplasia (dense fibrosis) which is a common characteristic of tumours. Furthermore, myofibroblasts are responsible for remodeling ECM and recruiting inflammatory cells and activating angiogenic programs (Tlsty & Coussens, 2006).

The carcinogenic process is a result of disturbances in cell division, cell growth and programmed cell death. The PI3K/AKT pathway plays a major role in all these processes. AKT activation contributes to a variety of oncogenic events, including inhibition of apoptosis, invasion, EMT, metastases and angiogenesis (Qiao *et al*., 2008). Our observation that POSTN induced AKT activation supports the notion that POSTN promotes ccRCC metastases. However, our research at this stage does not distinguish whether it is intracellular or extracellular POSTN that induces AKT activation in NIH3T3 cells. Additional research will be needed to address this issue.

5.4. Clinical Significance

ccRCC is the most predominant and aggressive form of renal cancer. The lethal factor for the disease is the progression of ccRCC towards metastasis. This situation is made worse due to the presence of a high rate (45%) of metastasized cases at initial diagnosis (Uchida *et al*., 2002). The metastatic ccRCC is resistant to chemotherapy and radiotherapy. However, our understanding regarding the mechanisms driving ccRCC progression to metastasis remains incomplete. Our research paves the way towards deepening our understanding of ccRCC metastasis. We demonstrate that ccRCC cells induce fibroblast cells to produce and secrete high levels of POSTN protein. This secreted POSTN protein in turn promotes ccRCC cell adhesion. Furthermore, stromal POSTN is abundant in the organ confined ccRCC and also the secondary organ, to which ccRCC metastasizes. These secondary organs do not normally express POSTN at high levels, suggesting a potential role for POSTN in ccRCC metastasis. In line with these results, ccRCC-induced stromal production of POSTN could potentially be targeted for ccRCC treatment. The communication from ccRCC to fibroblasts could be blocked so that the stromal cells cannot upregulate POSTN. However, this will first require us to identify the soluble factors generated by ccRCC cells which induce fibroblasts to produce POSTN. The secretion of POSTN by fibroblast cells could also be targeted. Another potential option is the utilization of neutralizing POSTN antibodies to bind extracellular POSTN. POSTN targeting in ccRCC is a promising avenue for therapy in order to prevent ccRCC progression. Future research will be needed to conclusively determine the role of POSTN in ccRCC metastasis.

VI. REFERENCES

Aboussekhra A. (2011). Role of cancer-associated fibroblasts in breast cancer development and prognosis. *Int J Dev Biol*, 55, 841-849.

Amin MB., Amin MB., Javidan, J., Tamboli, P., Stricker, H., Venturina,. et al. (2002). Prognostic Impact of Histologic Subtyping of Adult Renal Epithelial Neoplasms An Experience of 405 Cases. *The American Journal of Surgery*,26(3), 281-291.

Bao, S., Ouyang, G., Bai, X., Huang, Z., Ma, C., Liu, M., et al. (2004). Periostin potently promotes metastatic growth of colon cancer by augmenting cell survival via the Akt/PKB pathway. *Cancer cell*, 5(4), 329-39.

Baril, P., Gangeswaran, R., Mahon, PC., Caulee, K., Kocher, H.M., Harada, T., et al. (2007). Periostin promotes invasiveness and resistance of pancreatic cancer cells to hypoxia-induced cell death: role of the beta4 integrin and the PI3k pathway, *Oncogene*, 26, 2082-94.

Ben, Q.-wen, Zhao, Z., Ge, S.-fang, Zhou, J. I. E., Yuan, F. E. I., & Yuan, Y.-zong. (2009). Circulating levels of periostin may help identify patients with more aggressive colorectal cancer. *International Journal of Cancer*, 821-828.

Bhuvarahamurthy, V., Kristiansen, GO., Johannsen, M., Loening, SA., Schnorr, D., Jung, K., *et al.* (2006).In situ gene expression and localization of metalloproteinases MMP1, MMP2, MMP3, MMP9, and their inhibitors TIMP1 and TIMP2 in human renal cell carcinoma. *Oncol Rep,* 15 (5)**,** 1379-84.

Brant,W., Helms, C. Fundamentals of diagnostic radiology. (1999). Philadelphia, Pa: Lippincott, Williams & Wilkins.

Cantley LC. (2002). The phosphoinositide 3-kinase pathway. *Science*, 296 (5573), 1655–1657.

Carmeliet, P., & Jain, R. K. (2000). Angiogenesis in Cancer and Other Diseases. *Nature*, 407(6801), 249-257.

Castronovo, V., Waltregny, D., Kischel, P., Roesli, C., Elia, G., Rybak, J.-n, et al. (2006). A Chemical Proteomics Approach for the Identification of Accessible Antigens Expressed in Human Kidney Cancer *. *Molecular & Cellular Proteomics*, 2083-2091.

Cheville, J. C., Lohse, C. M., Zincke, H., D, P., Weaver, A. L., & Blute, M. L. (2003). Comparisons of Outcome and Prognostic Features Among Histologic Subtypes of Renal Cell Carcinoma. *American Journal of Surgery, The*, 27(5), 612-624.

Choyke, P. L., Glenn, G. M., Walther, Mcclellan M, Zbar, B., & Linehan, W. M. (n.d.). State of the Art Radiology Hereditary Renal Cancers 1. *Radiology*, 33-46.

Clifford, S. C., Prowse, a H., Affara, N. a, Buys, C. H., & Maher, E. R. (1998). Inactivation of the von Hippel-Lindau (VHL) tumour suppressor gene and allelic losses at chromosome arm 3p in primary renal cell carcinoma: evidence for a VHL-independent pathway in clear cell renal tumorigenesis. *Genes, chromosomes & cancer*, 22(3), 200-9.

Contié, S., Voorzanger-Rousselot, N., Litvin, J., Clézardin, P., Garnero, P. (2011). Increased expression and serum levels of the stromal cell-secreted protein periostin in breast cancer bone metastases. *Int J Cancer,* 128, 352-60.

Desmoulière, A., Guyot, C., & Gabbiani, G. (2004). The stroma reaction myofibroblast :a a key player in the control of tumor cell behavior. *Recherche*, 517, 509-517.

Fergany, A., Hafez, KS., Novick, AC. (2000). Long-term results of nephron sparing surgery for localized renal cell carcinoma: 10-year followup. *J Urol* ,163, 442–445.

Fujimoto, K., Kawaguchi, T., Nakashima, O., Ono, J., Ohta, S., Kawaguchi, A., et al. (2011). Periostin, a matrix protein, has potential as a novel serodiagnostic marker for cholangiocarcinoma. *Oncology reports*, 25(5), 1211-6.

Fuhrman SA, Lasky LC, Limas C. (1982). Prognostic signifi cance of morphologic parameters in renal cell carcinoma. *Am J Surg Pathol*, 655–63.

Gillan, L., Matei, D., Fishman, DA.,Gerbin, CS., Karlan, BY., Chang, DD. (2002). Periostin secreted by epithelial ovarian carcinoma is a ligand for alpha(V)beta(3) and alpha(V)beta(5) integrins and promotes cell motility. *Cancer Res*, 62, 5358-64.

Grignon, DJ., Eble, JN., Bonsib, SM., et al. (2004).Clear cell renal cell carcinoma. *Lyon (France): IARC Press*, 2004.

Grignon, D. J., & Che, M. (2005). Clear Cell Renal Cell Carcinoma. *Cancer*, 25, 305-316.

Hanamura, N., Yoshida, T., Matsumoto, E., Kawarada, Y., Sakakura, T. (1997). Expression of fibronectin and tenascin-C mRNA by myofibroblasts, vascular cells and epithelial cells in human colon adenomas and carcinomas. *Int J Cancer*, 73(1), 10-15.

Hofmeister, V., Schrama, D., Becker, JC. (2008). Anti-cancer therapies targeting the tumor stroma. *Cancer Immunol Immunother* , 57, 1–17.

Horiuchi, K., Amizuka, N., Takeshita, S., Takamatsu, H., Katsuura, M., Ozawa, H., et al. (1999). Identification and Characterization of a Novel Protein , Periostin , with Restricted Expression to Periosteum and Periodontal Ligament and Increased Expression by Transforming Growth Factor . *Journal of Bone and Mineral Research*, 14(7).

Iozzo, R. V. (1995). Tumor stroma as a regulator of neoplastic behavior. *Lab Investig,* 73, 157–160.

Isono, T., Kim, CJ., Ando, Y., Sakurai, H., Okada, Y., Inoue, H. (2009). Suppression of cell invasiveness by periostin via TAB1/TAK1. *Int J Oncol*, 35,425-32.

Javidan, J., Stricker, H. J., Tamboli, P., Amin, M. B., Peabody, J. O., Deshpande, A. (1999). Prognostic significance of the 1997 TNM classification of renal cell carcinoma. *J Urol*, 162,281–91.

Jemal, A., Thomas, A., Murray, T & Thun M. (2002). Cancer statistics 2002. *CA Cancer J Clin* 2002, 52(1), 23-47.

Jemal, A., Siegel, R., Ward E., Hao, Y., Xu, J., Murray, T., & Thun MJ . (2008). Cancer statistics 2008. *CA Cancer J Clin* 2008, 58, 71-96.

Kattan, MW., Reuter, V., Motzer, RJ., et al. (2001). A postoperative prognostic nomogram for renal cell carcinoma. *J Urol,166*, 63–7.

Kii, I., Nishiyama, T., Li, M., Matsumoto, K.-ichi, Saito, M., Amizuka, N., et al. (2010). Incorporation of Tenascin-C into the Extracellular Matrix by Periostin Underlies an Extracellular Meshwork Architecture . *Journal of Biological Chemistry*, 285(3), 2028 - 2039.

Kim, C. J., Yoshioka, N., Tambe, Y., Kushima, R., Okada, Y., & Inoue, H. (2005). Periostin is down-regulated in high grade human bladder cancers and suppresses in vitro cell invasiveness and in vivo metastasis of cancer cells. *Cancer Cell*, 58, 51-58.

Kim, W. Y., & Kaelin, W. G. (2004). Role of VHL gene mutation in human cancer. *Journal of clinical oncology : official journal of the American Society of Clinical Oncology,* 22(24), 4991-5004.

Kojima, Y., Acar, A., Eaton, E.N., Mellody, K.T., Scheel, C., Ben-Porath, I., et al.(2010). Autocrine TGF-beta and stromal cell-derived factor-1 (SDF-1) signaling drives the evolution of tumor-promoting mammary stromal myofibroblasts. *Proc Natl Acad Sci USA* 107, 20009-20014.

Kovacs, G., & Frisch, S. (1989). Clonal chromosome abnormalities in tumor cells from patients with sporadic renal cell carcinomas. *Cancer Res*, 49(3), 651-659.

Kudo, A. (2011). Periostin in fibrillogenesis for tissue regeneration: periostin actions inside and outside the cell. *Cell Mol Life Sci,68*, 201-207.

Lam, J. S., Leppert, J. T., Figlin, R. A., & Belldegrun, A. S. (2005). Surveillance Following Radical or Partial Nephrectomy for Renal Cell Carcinoma. *Current Urology Reports*.

Landis, S. H., Murray, T., Bolden, S. and Wingo, P. A. (1999). Cancer statistics, 1999. *CA Cancer J lin,* 49 (8).

Langley, R. R., & Fidler, I. J. (2012). interactions in metastasis to different organs. *International Journal*, 128(11), 2527-2535.

Lee SB & Haber DA. (2001).Wilms tumor and the WT1 gene. *Exp Cell Res*. 264, 74-99.

Levy, DA., Slaton, JW., Swanson, DA., Dinney, CP. (1998). Stage specific guidelines for surveillance after radical nephrectomy for local renal cell carcinoma. *J Urol*, 159, 1163-7.

Lin, SP., Bierhals, A., & Lewis, FS. (2007). Best Cases from the AFIP. *JAMA*, 1801-1807.

Linehan, W. M., Zbar, B. and Klausner, R. D. (2001). Renal carcinoma. In: *The Metabolic & Molecular Bases of Inherited Disease, 8th ed*, Edited by C. R. Scriver, A. L. Beaudet, D. Valle and W. S. Sly and New York: McGraw-Hill, 907–929.

Linehan, W. M., Walther, M. M., & Zbar, B. (2003). The genetic basis of cancer of the kidney. *The Journal of urology*, 170(6 Pt 1), 2163-72.

Linehan, W., Srinivasan, R., & Schmidt, L. (2010). The genetic basis of kidney cancer: a metabolic disease. *Nature Reviews*, 7, 277-285.

Liu, JH., Yang, MH., Fan, FS., Yen, CC., Wang, WS., Chang, YH., et al. (2001). Tamoxifen and colchicine-modulated vinblastine followed by 5-fluorouracil in advanced renal cell carcinoma: a phase II study. *Urology,* 57, 650–654.

Maher, E.R., & Kaelin, W.G. (1997). von Hippel-Lindau disease. *Medicine.* 76, 381-391.

Malanchi, I., Martinez, AS., Susanto, E., Peng, H., Lehr, H.-anton, & Delaloye, J.-francois. (2012). Interactions between cancer stem cells and their niche govern metastatic colonization. *Nature*, 481.

Martinez, a, Fullwood, P., Kondo, K., Kishida, T., Yao, M., Maher, E. R., et al. (2000). Role of chromosome 3p12-p21 tumour suppressor genes in clear cell renal cell carcinoma: analysis of VHL dependent and VHL independent pathways of tumorigenesis. *Molecular pathology : MP*, 53(3), 137-44.

Michaylira, C. Z., Wong, G. S., Miller, C. G., Michaylira, C. Z., Wong, G. S., Miller, C. G., et al. (2010). Periostin , a Cell Adhesion Molecule , Facilitates Invasion in the Tumor Microenvironment and Annotates a Novel Tumor-Invasive Signature in Esophageal Cancer Periostin , a Cell Adhesion Molecule , Facilitates Invasion in the Tumor Microenvironment and Annotates a Novel Tumor-Invasive Signature in Esophageal Cancer. *Cancer Research*, 70, 581-592.

Mickisch, G. H., & Hospital, A. (1994). Chemoresistance of Renal Cell Carcinoma. *World Journal of Urology*, 12 (4) 214-223.

Morra, L., Rechsteiner, M., Casagrande., S., Duc Luu, V., Santimaria, R., Diener, PA., et al. (2011). Relevance of periostin splice variants in renal cell carcinoma. *Am J Pathol*, 179 (3), 1513-21.

Morra, L., & Moch, H. (2011). Periostin expression and epithelial-mesenchymal transition in cancer : a review and an update. *Virchows Archive*, 465-475.

Mueller, M. M., & Fusenig, N. E. (2004). REVIEWS FRIENDS OR FOES — BIPOLAR EFFECTS OF THE TUMOUR STROMA. *Nature*, 4.

Nelson, E. C., Evans, C. P., & Jr, P. N. L. (2007). Renal cell carcinoma : Current status and emerging therapies, 299- 313.

Nishiyama, T., Kii, I., Kashima, TG., Kikuchi, Y., Ohazama, A., Shimazaki, M., et al. (2011). Delayed re-epithelialization in periostin-deficient mice during cutaneous wound healing. *Plos ONE*, 6(4).

Norris, R. A., Damon, B., Mironov, V., Kasyanov, V., Moreno-rodriguez, R., Trusk, T., et al. (2012). NIH Public Access. *Cell*, 101(3), 695-711.

Orecchia, P., Conte, R., Balza, E., Castellani, P., Borsi, L., Zardi, L., et al. (2011). Identification of a novel cell binding site of periostin involved in tumour growth. *European Journal of Cancer*, 47(14), 2221-2229.

Prasad, SR., Humphrey, PA., Catena, JR., et al. (2006). Common and uncommon histologic subtypes of renal cell carcinoma: imaging spectrum with pathologic correlation. *RadioGraphics*, 26, 1795–1806; discussion 1806–1810.

Prenen, H., Gil, T., & Awada, A. (2009). New therapeutic developments in renal cell cancer. *Critical Reviews in Oncology/Hematology*, 69, 56-63.

Puppin, C., Passon, N., Frasca, F., Vigneri, R., Tomay, F., Tomaciello, S., et al. (2011). In thyroid cancer cell lines expression of periostin gene is controlled by p73 and is not related to epigenetic marks of active transcription. *System*, 34, 131-140.

Qiao, M., Sheng, S., & Pardee, A. B. (2008). Metastases and AKT Activation. An Overview of the Significance of AKT in Tumor Metastases. *Cell Cycle*, 2991-2996.

Rønnov-Jessen, L., Petersen, OW., Koteliansky, VE., Bissell MJ. (1995). The origin of the myofibroblasts in breast cancer: recapitulation of tumor environment in culture unravels diversity and implicates converted fibroblasts and recruited smooth muscle cells. *J Clin Invest*, 95, 859–873.

Ruan, K., Bao, Æ. S., & Ouyang, Æ. G. (2009). The multifaceted role of periostin in tumorigenesis. *Cellular and Molecular Life Science*s, 66, 2219-2230.

Sasaki ,H., Roberts, J., ykins, D., Fujii, Y., Auclair, D., Chen, LB. (2002). Novel chemiluminescence assay for serum periostin levels in women with preeclampsia and in normotensive pregnant women. *Am J Obstet Gynecol* , 186, 103-108.

Shao, R., Bao, S., Bai, X., Blanchette, C., Anderson, R. M., Dang, T., et al. (2004). Acquired Expression of Periostin by Human Breast Cancers Promotes Tumor Angiogenesis through Up-Regulation of Vascular Endothelial Growth Factor Receptor 2 Expression. *Society*, 24(9), 3992-4003.

Soltermann, A., Tischler, V., Arbogast, S., Weder, W., Moch, H., & Kristiansen, G. (2008). Prognostic Significance of Epithelial-Mesenchymal and Mesenchymal-Epithelial Transition Protein Expression in Non − Small Cell Lung Cancer Mesenchymal-Epithelial T ransition Protein Expression in Non Small Cell Lung Cancer. *Clinical Cancer Research*, 14(22), 1430-1437

Staal SP & Hartley JW. (1988). Thymic lymphoma induction by the AKT8 murine retrovirus. *J Exp Med*, 167 (3), 1259–1264.

Takayama, G., Arima, K., Kanaji, T., & Toda, S. (n.d.). (2006). Periostin : A novel component of subepithelial fibrosis of bronchial asthma downstream of IL-4 and IL-13 signals. *Clinical Immunology*, 98-104.

Takeshita, S., Kikuno, R., Tezuka, K.-ichi, & Amannt, E. (1993). Osteoblast-specific factor 2 : cloning of a putative bone adhesion protein with homology with the insect protein fasciclin I, *278*, 271-278.

Tilman, G., Mattiussi, M., Brasseur, F., van Baren,V., Decottignies,A.(2007). Human periostin gene expression in normal tissues, tumors and melanoma: evidences for periostin production by both stromal and melanoma cells. *Molecular Cancer*, 6(80).

Tischler, V., Fritzsche, F. R., Wild, P. J., Stephan, C., Seifert, H.-H., Riener, M.-O., et al. (2010). Periostin is up-regulated in high grade and high stage prostate cancer. *BMC cancer*, *10*, 273.

Tlsty, T. D., & Coussens, L. M. (2006). Tumor Stroma and Regulation of Cancer Development. *Development*, 119-150.

Tsunoda, T., Furusato, B., Takashima, Y., Ravulapalli, S., Dobi, A., Srivastava, S., et al. (2009). The increased expression of periostin during early stages of prostate cancer and advanced stages of cancer stroma. *Prostate*, 69(13), 1398-403.

Tuxhorn, JA., Ayala, GE., Smith, MJ., Smith, VC., Dang ,TD., Rowley DR. (2002). Reactive stroma in human prostate cancer: induction of myofibroblast phenotype and extracellular matrix remodeling. *Clin Cancer Res* ,8, 2912–2923.

Uchida, K., Miyao, N., Masumori, N., Takahashi, A., Oda, T., Yanase, M., et al. (2002). Recurrence of renal cell carcinoma more than 5 years after nephrectomy. *Int J Urol*. 9, 19-23.

Utispan, K., Thuwajit, P., Abiko, Y., Charngkaew, K., & Paupairoj, A. (2010). Gene expression profiling of cholangiocarcinoma- derived fibroblast reveals alterations related to tumor progression and indicates periostin as a poor prognostic marker. *Molecular Cancer*, 1-20.

Vignot, S., Faivre, S., Aguirre, D., & Raymond, E. (2005). mTOR-targeted therapy of cancer with rapamycin derivatives. *Annals of oncology : official journal of the European Society for Medical Oncology / ESMO*, 16(4), 525-37.

Vivanco, I., Sawyers, CL. (2002) The phosphatidylinositol 3-kinase AKT pathway in human cancer. *Nat Rev Cancer,* 2(7), 489–501.

Wang, Z., & Ouyang, G. (2012). Previews Periostin : A Bridge between Cancer Stem Cells and Their Metastatic Niche. *Stem Cell*, 10(2), 111-112.

Weidner, N., Semple, J.P., Welch, W.R., & Folkman, J. (1991).Tumor angiogenesis and metastasis correlation in invasive breast carcinoma. *N. Engl. J. Med*, 324, 1–8.

Yagoda A., Abi-Rached B., Petrylak D. (1995). Chemotherapy for advanced renal-cell carcinoma: 1983-1993. *Semin Oncol*, 22, 42-60.

Yamaguchi, H., Wyckoff, J., & Condeelis, J. (2005). Cell migration in tumors. *Current Opinion in Cell Biology*, 559-564.

Zhang, Y., Zhang, G., Li, J., Tao, Q., & Tang, W. (2010). The expression analysis of periostin in human breast cancer. *The Journal of surgical research*, 160(1), 102-106.

Zhu, M., Fejzo, M. S., Anderson, L., Dering, J., Ginther, C., Ramos, L., et al. (2010). Gynecologic Oncology Periostin promotes ovarian cancer angiogenesis and metastasis. *Gynecologic Oncology*, 119(2), 337-344.

Zigrino, P., Löffek, S., & Mauch, C. (2005). Tumor – stroma interactions : their role in the control of tumor cell invasion, 87, 321-328.